NASA TECHNICAL MEMORANDUM

NASA TM 73708

NASA TM 73708

EFFECTS OF SIMULATED FLIGHT ON FAN NOISE SUPPRESSION

by Marcus F. Heidmann and Donald A. Dietrich
Lewis Research Center
Cleveland, Ohio 44135

TECHNICAL PAPER to be presented at the
Fourth Aeroacoustics Conference
sponsored by the American Institute of Aeronautics and Astronautics
Atlanta, Georgia, October 3-5, 1977

EFFECTS OF SIMULATED FLIGHT ON FAN NOISE SUPPRESSION

Marcus F. Heidmann* and Donald A. Dietrich**
National Aeronautics and Space Administration
Lewis Research Center
Cleveland, Ohio 44135

Abstract

Attenuation properties of 3 treated fan inlets were evaluated in the NASA-Lewis Anechoic Wind Tunnel using a subsonic tip speed, 50.8 cm-diameter model fan. Tunnel flow simulated the inflow clean-up effect on source noise observed in flight and allowed observation of the blade passage frequency tone cut-off phenomenon. Acoustic data consisted of isolated inlet noise measured in the far field at two fixed positions and with traverses at 4 frequencies. Attenuation and source noise properties with and without flight simulation are compared and discussed. Averaged attenuation properties showed relative agreement of the inlets with their design intent, however, tunnel flow significantly affected the attenuation spectra. With no tunnel flow the strong blade passage tone was more highly attenuated than the adjacent broadband noise. With tunnel flow, when cut-off was observed, the attenuation at the tone frequency was comparable to that for broadband noise. Tunnel flow generally increased by several dB the maximum attenuation occurring at midfrequencies of the attenuation spectra. The combined effect of tunnel flow on attenuation and source noise, however, generally resulted in suppressed fan noise levels throughout the spectra that were as low or lower than those obtained statically. Tunnel flow caused some substantial directivity variations that are interpreted as acoustic mode changes, with tunnel flow generally reducing the proportion of modes near cut-off. Narrowband spectra reveal a multiplicity of shaft order tones that are interpreted in terms of rotor imperfections, inflow distortions and modal content. A tone-like high frequency noise was identified as self-noise from the honeycomb/perforate treatment used in two of the inlets.

Introduction

Forward flight is known often to reduce or alter the noise generated by the bypass fan of an aircraft engine compared to that observed during ground-static operation as exemplified in ref. 1. The changes in fan noise are attributed to the cleaner in-flow that occurs during flight than on the ground. Considerable effort has been expended to evaluate and understand these ran source noise changes because of the impact flight effects can have on the development of quieter aircraft engines. Operational aircraft, however, almost invariably employ acoustically treated fan inlets and exhaust ducts. Equally important to source noise changes, therefore, is the response of acoustic treatment to the changes in source noise incurred during flight. Noise suppression can be highly sensitive to changes in the propagating patterns that exist in a treated duct.[2] The question of treatment effectiveness during flight compared to that during ground static testing, however, has received little attention.

*Aerospace Research Engineer, V/STOL and Noise Division.

**Aerospace Research Engineer, Wind Tunnel & Flight Division.

The purpose of this paper is to report the acoustic results of some simulated-flight tests of a model fan with treated inlets. The tests were conducted in the NASA-Lewis 9×15 Anechoic Wind Tunnel. The fan stage was designed for blade passage tone cut-off due to rotor/stator interactions according to the Tyler-Sofrin theory.[5] Previous acoustic tests in the tunnel with the model fan[3,4] showed that flight effects on fan source noise were simulated at tunnel flows above about 20 M/sec. The prominent features of the simulated-flight noise that distinguish it from static noise were (1) a substantially reduced level of the fundamental blade passage tone, (2) reduced time unsteadiness of a tone harmonic level and (3) a distinctively lobed directivity of a propagating tone harmonic. In the current study three treated inlets were tested with and without tunnel flow at three subsonic fan speeds.

With regard to acoustic treatment design, a honeycomb backing with perforated faceplate was used for two of the inlets and bulk absorber material with a perforated faceplate was used for the other inlet. The inlets had been designed for and statically tested with a similar model fan[6] in support of a quiet engine (QCSEE) development program. The designs do not reflect any specific attempt to capitalize on the differences in flight and ground-static fan source noise. The wind tunnel results, however, are believed to be indicative of the suppression changes that might be expected during flight for currently used treated inlets.

Test Facilities and Procedure

The wind tunnel facilities, model fan and instrumentation are identical to that described for the previous tests[3,4]. Figure 1 shows the model fan installed in the anechoic test section of the wind tunnel. Acoustic measurements are limited to fan inlet noise by ducting the fan exhaust outside the test section through the acoustically treated exhaust stack. The rotatable boom microphone shown in the photograph was located 3.6 fan diameters from the center of the inlet face and was the primary source of acoustic data. Traversing measurements through the fan inlet quadrant were recorded on-line for 1/3-octave band signals at 1, 1-1/2, 2 and 2-1/2 times the blade passage frequency for each test condition. Acoustic signals were also tape recorded for later reduction at fixed boom microphone position of 60 and 90 degrees from the inlet axis.

The reported acoustic data are generally limited to frequencies above 1000 Hz because of tunnel flow noise and anechoic properties of the test section. The data from the on-line traversing measurements were generally adjusted to that measured at fixed position in the traversing plane. The absolute accuracy at the fixed positions based on direct calibration of the microphones was expected to be ±1 dB. Analyses of some supplemental calibration data, however, in some instances indicated absolute level differences of about 2 dB between tests made on different days. The supplemental data consisted of

the measured broadband noise of a small calibrated air jet that was introduced between series of tests and the very low frequency noise for each test condition that appeared insensitive to the inlet configuration being tested. Data corrections were made on the basis of the supplemental calibration results for certain test days. Specifically, the measured noise levels were reduced by 2 dB for the hardwall inlet tested without tunnel flow and for inlet A (described later) tested both with and without tunnel flow.

Some of the design properties of the 50.8 cm (20 in.) diameter subsonic tip-speed fan stage are given in Table I. A variable pitch rotor (NASA-Lewis Rotor-55) is used in this stage at its design blade angle setting. According to the Tyler-Sofrin theory, the vane/blade ratio of 1.67 shown in Table I produces cut-off of the fundamental blade passage frequency (BPF) tone from rotor/stator interactions below about 107% of the design speed. The second harmonic should not be cut-off above very low fan speeds but should be limited to a few propagating modes. In the previous tests[3,4], fundamental tone cut-off at tunnel flows above about 20 m/sec was observed. Tunnel flow reduced the time unsteadiness of the second harmonic tone and a distinctively lobed far-field directivity pattern was observed. No dramatic increase in the fundamental tone level was noted, however, at fan speeds above the cut-off speed.

In the previous study[3,4] tests were made with a hardwall untreated fan inlet for parametric variations in fan speed, fan loading, inlet angle of attack and tunnel velocity. For this study, tests were made with the hardwall and three treated inlets at 95, 106 and 110% of fan design speed at both 0 and 43 m/sec tunnel velocities. Zero angle of attack was used. The fan speed changes, however, were made along an operating line that differed from that used in the previous study. Higher fan speeds required for the previous study necessitated an operating line that avoided choked fan flow conditions as is evident in the fan performance map shown in figure 2.

Fan Inlet Configurations

Design properties of the acoustically treated inlets and the reference hard wall inlet are shown in Table II. The basic aerodynamic design is identical for all the inlets and is representative of a conventional flight type inlet having a throat Mach number of 0.60. The acoustic treatment used in the inlets consisted of two types. A honeycomb structure with perforated faceplate was used for Inlets A and A(mod) and a bulk absorber (Scottfelt) with perforated faceplate was used for Inlet B. Inlet A(mod) is Inlet A with the forward low frequency segment of the 3 segment configuration taped to make it inactive. Aerodynamic tests were conducted with these and other inlets in a separate study.[7] The results showed inlet flow to be attached and a pressure recovery above 0.99 at the conditions for the current tests. Although pressure recovery was always high, there was some evidence of decreased pressure recovery with increased open area ratio of the perforated faceplate with Inlet B exhibiting the lowest pressure recovery.

The treated inlets used in this study were designed and previously tested by the General Electric Co. in support of the NASA-Lewis QCSEE (Quiet Clean Short-Haul Experimental Engine) Program.[6] In that study, a 50.3 cm (20-in.) diameter fan stage designated the QCSEE-simulator was used. This fan stage had a higher design tip speed (306.3 m/sec), rotor blade number (18) and blade/vane ratio (1.83) than that used in the current study. Fundamental tone cut-off for this fan stage would be expected below about 92% of design speed with clean inflow. Static acoustic tests were made with this fan in an anechoic chamber. The treated sections of the inlet, however, were tested with an aeroacoustic (modified bellmouth) rather than the flight-type inlet used in the current study. Some comparisons with these previous results will be made.

The design of the acoustic treatment was intended to minimize the perceived noise levels of a full-scale version of the QCSEE-Simulator fan stage. The tuning frequencies listed in Table II reflect this design objective. The inlet designs, therefore, were not intended to meet any specific noise objective for the model or full-scale version of the Rotor-55 fan stage. They are used in this study because they represent state-of-the-art treated inlets that are useful to explore the effects of flight on noise suppression.

The tuning frequencies listed for these inlets in Table II are actually the design frequencies used to specify the treatment configuration giving optimum suppression for a specific duct acoustic mode. The lowest radial order of the 10th order spinning lobe mode was used to design the honeycomb/perforated plate configurations.[6] For other modes the maximum but not necessarily optimum suppression will occur at a different frequency from the values listed. The maximum suppression for a mixture of modes characteristic of broadband noise would generally be expected to occur at a different frequency than that shown in Table II. The uncertainties that exist at this time in specifying the acoustic modes that are present at significant levels severely restricts any prediction of suppressor behavior expected from a change in source noise due to flight, operating conditions or fan configuration.

The tuning frequency for the bulk absorber treatment used for Inlet B was assigned broadband properties in the previous study.[6] The depth and compactness of the bulk absorber material, however, does determine the frequency region where it is most effective. For the material used in Inlet B the suppression is expected to center around 5000 Hz and encompass the same frequency range expected from the three treated segments used in Inlet A. In other words, Inlets A and B had similar noise suppression design objectives but differed in treatment structure.

Inlet A(mod) was tested in an attempt to evaluate the effectiveness of the forward segment of treatment in Inlet A. The leading edge of this segment approaches the inlet throat and is in a region of high flow diffusion where the behavior of acoustic treatment is questionable. A comparison of the results of Inlet A with that of Inlet A(mod), where the forward segment was taped, was expected to give some insight into the behavior of treatment in a diffusion zone.

Modal Propagation

Modal propagation is the classical method used to analyze and to characterize fan noise generation

and propagation. Many of the results of this study will be interpreted in terms of acoustic mode properties extracted from previous analyses. Some of these acoustic mode properties will be discussed in this section.

Tone noise is of primary interest. Tone noise, however, is not limited to the blade passage frequency and its harmonics but also includes shaft order tones (tones at the fan shaft rotational frequency and its harmonics). Shaft order tones were evident in the spectra previously reported for the fan[4] and will be shown to be even more prominent at the fan operating conditions used in this study. Figure 3 is typical of the narrowband spectra obtained with the fan during static test conditions. Nearly all of the shaft order tones can be identified in the spectra.

The modal propagation that can be associated with these shaft order forms will be based on the analyses of previous investigators[8-10]. Tone noise is assumed to be generated by the interaction of rotor wakes with the stator vanes and the interaction of the rotor with inflow distortions. The acoustic modes generated consist of plane waves and circumferentially lobed patterns that spin both with and counter to the rotor. The spinning modes essentially propagate in the fan inlet along helical paths. When the helical angle of the propagation path is large the mode is considered highly propagating. The degree of propagation decreases with a decrease in the helical angle. The mode does not propagate or is denoted as cut-off when the angle is zero. A mixture of propagating modes, therefore, can range from highly propagating to near cut-off modes.

Figure 4 displays acoustic modes by which the shaft order tones can propagate through the inlet. The circumferential spinning order, m, (number of lobes) of propagating patterns allowable at each shaft order (frequency) are shown for the 106% of design fan speed. The value of m is an integer and the values for which at least the lowest radial order of the spinning mode can propagate are displayed within the figure. Negative values of m denote modes rotating counter to that of the rotor. The highest value of m at each shaft order (the extremities of the numerical pattern) are near cut-off and the lowest values of m are highly propagating modes. The zero order mode is the plane wave and most highly propagating for each of the family of modes. When the mode is highly propagating the higher radial order modes with the same circumferential order m can also propagate and considerably increase the population of modes beyond that shown in figure 4.

The construction of figure 4 is based on an analysis where the circumferential order of the acoustic mode (number of lobes), m, is given by the sum and difference of any circumferential order of the rotor, n, and any circumferential order, k, of a fixed flow field pattern in the duct, $m = (n \pm k)$. The criteria for propagation depends on the actual rotational speed of this mode and its eigenvalue. The evaluation for propagation was made at the fan inlet throat and includes the effect of flow on propagation. The Tyler-Sofrin theory[5] for rotor/stator interactions is a special case for a perfect rotor and perfect stator where the value of n and k are integer multiples of the number of rotor and stator blades, respectively. The perfect rotor and stator modes with clean (distortionless) inflow are shown circled in figure 4. No mode is circled for the BPF (15th shaft order) because it is cut-off at the inlet throat for this fan speed and only the harmonics of the BPF tone can propagate. Intermediate shaft order tones cannot arise from a perfect rotor.

The effect of inflow disturbances on mode generation depends on the circumferential orders (similar to harmonic component) needed to depict a fixed inflow distortion. For this case, any integer value of the circumferential order k is possible. The possible acoustic modes obtained with a perfect rotor and a fixed inflow distortion are shown by the values enclosed by the vertically aligned rectangles. These modes are also possible with an imperfect stator row where the vane spacing is not equal and k cannot be limited to integer multiples of the number of vanes. The inflow distortion or imperfect stator with a perfect rotor increases the number of possible modes at the BPF and its harmonics but does not account for other shaft order tones.

For clean inflow, a family of shaft order tones at other than the BPF and its harmonics is only possible with an imperfect rotor (unequal blades spacing or blade angles). The diagonally aligned rectangles shown in figure 4 enclose the probable modes for the interactions of an imperfect rotor with a perfect stator and clean inflow. All shaft order tones higher than the BPF are shown to be possible for this fan at 106% of design speed. The number of possible modes at each shaft order, however, is limited to a few spinning orders. Inflow distortions or an imperfect stator are needed to interact with the imperfect rotor to increase the number of possible modes. Under such conditions all modes shown in figure 4 are possible.

On the basis of this modal analysis and the evidence of a multiplicity of shaft order tones in the spectra of figure 3, it is concluded that the tests in this study were conducted with an imperfect rotor. The variable blade angle design features of the rotor and the possibility of misadjustments may have contributed to the imperfection although evidence of imperfect rotors is also frequently observed with fixed designs [8,9,11]. It can also be concluded from figure 4 that the imperfect rotor interacts with an inflow distortion or an imperfect stator. The shaft order tones evident below the BPF tone are only possible under such conditions. The strong BPF tone is also indicative of inflow disturbances. All tones, therefore, can be presumed to be a mixture of modes spinning in both directions and ranging from near cut-off to the highly propagating plane wave. The number of modes in the mixture increases with shaft order.

Although figure 4 characterizes the modes associated with shaft order tones it is also indicative of the modal content of any broadband noise. The propagation of broadband noise is not limited to shaft order tones but can occur at all intermediate frequencies. At the shaft order frequencies the probable broadband noise modes are identical to that for the shaft order tones. At intermediate frequencies the broad band modes are intermediate to that for the adjacent shaft order tones shown in figure 4. Broadband noise, therefore, can also consist of a modal mixture ranging from highly propagating to near cut-off modes.

The propagation of modal mixtures was analyzed by Saule and Rice[12,13] and generalities were expressed regarding far-field directivity patterns. A modal mixture consisting of equal energy in all possible modes at a given frequency can be assumed as a reference case. If the energy distribution is more heavily weighted toward the highly propagating modes the directivity at low angles from the fan inlet axis increases at the expense of that near the plane of the fan. Conversely, the directivity near the plane of the fan is increased by weighting the mixture with modes near cut-off. Changes in directivity patterns, therefore, can be indicative of changes in the energy distribution of modal mixtures. The directivity pattern of a modal mixture is relatively uniform and does not exhibit the distinctive lobed pattern[5] of a single mode. A lobed far field directivity pattern is only exhibited when the acoustic energy is concentrated in relatively few acoustic modes.

The attenuation properties of modal mixtures by inlet suppressors were also examined by Rice[14] and generalities expressed regarding far-field propagation properties. For a modal mixture at a given frequency, the attenuation of the modes near cut-off is usually much larger than that for the highly propagating modes. The attenuation observed in the far-field as a function of angle from the fan axis, therefore, can be indicative of the modal mixture generated by the source. If the attenuation increases with an increase in the angle from the inlet axis, modes near cut-off may be prevalent in the modal mixture. If the attenuation is relatively uniform, the modal mixture may be dominated by the highly propagating modes. These generalities may be obscured by other possible complexities of duct attenuation and far field directivities but provide some insight into the modal mixture present in the propagating noise.

These selected generalities of modal propagation will be used in the subsequent discussion of both the source noise and treated inlet results.

Source Noise Characterization

The effect of flight on the performance of inlet suppressors is intimately involved with the effect of flight on fan source noise because acoustic treatment is expected to be primarily sensitive to changes in the modal patterns that enter a treated duct. Although these modal patterns can seldom be specifically identified, a characterization of the spectral and directivity properties of the source noise may provide some insight into the variability of modal propagation that can be experienced. In this section, test results obtained with the hardwall untreated inlet will be presented. They will be used to not only identify source noise properties but also provide the datum used to evaluate attenuation levels for the treated inlets.

One-Third Octave Band Spectra

The effect of tunnel flow on the 1/3-octave band spectral properties were previously reported.[3,4] These results, however, were obtained at fan operating conditions that differ from those used in this study. The differences in operating conditions are identified in the fan performance map shown in figure 2. A relatively low fan blade loading was used for the present study with the 110% of design fan speed condition lying close to the choked flow line. As previously reported[4], source noise changes are experienced with a change in blade loading.

The effect of tunnel flow on the 1/3-octave band spectra for the three fan speeds used in this study is shown in figure 5. The changes in spectral properties with tunnel flow are similar to those previously observed. The most prominent effect of tunnel flow is the reduced level or apparent elimination of the fundamental blade passage frequency (BPF) tone. This change in source noise is attributed to both the cut-off design feature of the fan stage and the cleaner fan inflow with tunnel flow.

Spectral changes at frequencies other than at the BPF are more evident at 90° than at 60° from the inlet axis. At the 90° position, high frequency noise is reduced by tunnel flow at all three speeds. As previously stated, a noise reduction in the plane of the fan may be indicative of a change in modal content. The change noted in figure 5 implies that tunnel flow reduced the proportion of modes near cut-off in the modal mixture. Additional evidence of such changes in source noise will be discussed later.

Directivity Patterns

The directivity patterns from the microphone traverses for the hardwall inlet obtained with and without tunnel flow are shown in figure 6 for the 106% of design fan speed. The patterns are similar to those reported and discussed previously.[3,4] The level of the BPF tone and the time unsteadiness of both the BPF and the 2XBPF tone are reduced by tunnel flow. The lobular directivity pattern for the 2 BPF tone with tunnel flow is less distinct than that previously observed[3] or that obtained at other fan speeds. It is indicative, however, of relatively fewer acoustic modes containing most of the acoustic energy. The noise at 1.5 and 2.5 times the BPF (presumed to be broadband noise) exhibits less unsteadiness and less change with tunnel flow. The unsteadiness of the tones under static test conditions is attributed to the interaction of the rotor with inflow disturbances intermittently ingested by the inlet. Tone source noise under static conditions is presumed to consist of a changing mixture of duct modes with any of the allowable propagating modes being probable. Time unsteadiness also increases the bandwidth of a tone because of the phase and frequency modulations that accompany time unsteadiness (random amplitude modulations of the tone).

The differences in the directivity patterns (flow minus no flow) are shown in figure 7 for the 3 fan speed conditions. The differences in level cannot be considered precise because of the unsteadiness of the recorded levels and accuracy limitations of the facility. The difference patterns, however, are similar at all fan speeds. Tunnel flow reduced the BPF tone about 10 dB at all inlet angles. The difference pattern for the 2XBPF tone varies with inlet angle because of the lobular pattern of this tone exhibited with tunnel flow. The average level of the 2XBPF tone did not change significantly although there is a reduction trend with increasing inlet angle. This result as previously discussed implies that the number of modes near cut-off have been reduced. As indicated in figure 4, modes near cut-off should be eliminated by inflow clean-up for an imperfect rotor and perfect stator. The noise at

1.5 BPF also exhibits a variation with inlet angle that implies a proportional reduction in modes near cut-off. The increased level exhibited at lower inlet angles, if reliably measured, indicates some increase in highly propagating modes. The noise at 2.5 BPF did not exhibit this increase at small angles. The trend shown for the 2.5 BPF level infers that tunnel flow enchances the number or level of modes propagating at about 60° from the inlet at the expense of modes near cut-off. These changes at 1.5 and 2.5 BPF (presumably broadband noise) are more pronounced than those observed for the fan operating line of the previous study.[3,4]

Any modal properties infered from 1/3 octave band data must be qualified because of the varied spectral structure that can occur within the 1/3-octave bandwidth. The following results obtained from narrow band spectral analyses of the data illustrates that the detailed spectral structure indeed is complex.

Narrowband Spectra

Narrowband spectra (25 Hz bandwidth) both with and without tunnel flow are shown in figure 8 for inlet angles of 60° and 90° and a fan speed of 106% of design. The property of these spectra of primary interest is the multiplicity of shaft order tones. The shaft order and the frequency for these tones are denoted by the abscissa in figure 8. The narrowband spectra for static conditions, as previously stated, are indicative of the imperfect rotor interacting with an inflow disturbance or with an imperfect stator. The shaft order tones evident at the very low orders are only possible under such conditions. The strong BPF tone is also indicative of inflow disturbances. All tones are presumed to be a mixture of modes shown in figure 4 with the number of modes in the mixture increasing with shaft order.

The spectra obtained with tunnel flow show a weak BPF tone and a variety of shaft order tones. The reduction in the BPF tone caused by tunnel flow is indicative of inflow clean-up. The weak tone may be due to either some residual inflow distortion or stator imperfections. The BPF tone, however, borders on cut-off and the weak tone may also indicate incomplete cut-off or the imprecision of the cut-off theory for a diffusing inlet. The variety of shaft order tones shown in the spectra with tunnel flow confirm that the rotor is imperfect. Tones at shaft orders lower than that for the BPF tone, however, are not evident as expected with clean inflow. On the basis of these spectral results the remaining shaft order tones are probably primarily confined to the acoustic modes associated with an imperfect rotor, perfect stator and clean inflow. The circumferential orders for these modes are identified in figure 4, however, the number of allowable modes is greater than that shown because higher radial order modes are also allowable for the lower circumferential orders.

The complexity of the modal propagation is further revealed by the point by point differences in narrowband spectra shown in figures 9 and 10. The spectral changes obtained with tunnel flow at 60° from the inlet are shown in figure 9. The reduction in level of the cluster of shaft order tones at the BPF is an expected result. At other frequency regions, however, some shaft order tones are significantly increased. The result implies that tunnel flow can significantly alter the source noise generation process and does not simply remove or reduce the noise caused by inflow disturbances.

The effect of tunnel flow on spectral properties at only one angular position must be interpreted with caution. Figure 10 illustrates the spectral changes in shaft order tones that can occur with angular position. The differences between the spectra at 60° and 90° from the inlet are shown for both static and tunnel flow conditions. The difference spectrum for the static test is relatively uniform compared to that with tunnel flow. The shaft order tones observed with tunnel flow in figure 10 appear highly variable with inlet angle. Such variability is expected when relatively few modes are propagating to give a highly lobular directing pattern.

Another characteristic of the source noise that may be significant to the interpretation of the inlet suppressor results is the extreme sensitivity of spectral properties to changes in operating conditions of this fan. Figure 11 shows the narrowband and 1/3-octave-band spectra at 60° from the inlet for two very closely spaced fan operating conditions with tunnel flow. The upper spectra in figure 11(a) is for the 106% speed condition previously shown in figure 7. The lower spectra is for the same fan speed except for a slight increase in loading obtained with a nozzle area change. The total pressure increase and the flow rate decrease for this condition are both less than 1/2 of 1%. These small changes, however, caused significant changes in the shaft order tones evident in the spectra of figure 11(a). The effect of the small operating condition change is particularly important because the total pressure losses inherent with treated inlets can affect operating conditions to the extent used in the illustration for figure 11. The introduction of a treated inlet, therefore, may significantly alter the source noise for this fan stage and a source noise description based on hardwall inlet results will not be as precise or accurate a reference condition for evaluating suppressor performance as desired.

This attempt to characterize the source noise has shown that a precise description, particularly with regard to the propagating acoustic modes, is not possible with the available data. The inflow clean-up obtained with tunnel flow has revealed that the source noise of a fan can exhibit an individualistic type of character that is usually obscured during static testing. The uniqueness of the configuration or the operating condition for the fan used in this study can only be assessed after a variety of fan designs have been tested under similar conditions.

Treated Inlet Results and Discussion

In this section the results obtained from tests with the treated inlets will be presented and the attenuation properties of the 3 inlets will be compared and discussed. The 1/3-octave band spectra results will be discussed first and the results from the 1/3-octave band directivity traverses and from narrowband spectral analyses will follow. Some comparisons with the results from previous tests with the inlets[6] will also be presented. Finally, the evidence of noise generated by the acoustic treatment will be discussed.

One-Third Octave Band Spectra

The 1/3-octave spectra at inlet angles of 60° and 90° measured with the 3 inlets installed on the fan are presented in figures 12-14. The results with and without tunnel flow are shown in each figure for comparative purposes. The most prominent effect of tunnel flow for all three inlets is the virtual disappearance of the BPF tone. This decrease in the BPF tone, of course, is primarily the result of a source noise change and not indicative of the suppressor performance that will be examined in more detail subsequently. Spectral differences with and without tunnel flow at other frequencies exhibit a more varied behavior.

There are several limitations to the results presented in figures 12-14. One is the malfunction of the boom microphone for inlet A(mod) when it was tested statically. The results shown for this condition were inferred from auxiliary microphones located in the test section ceiling. (The inferred level is the hardwall level of the boom microphone minus the attenuation of inlet A(mod) measured with the ceiling microphones.) The comparisons of levels with and without tunnel flow for Inlet A(mod) in figure 13, therefore, are questionable. Also, a tunnel noise floor may have influenced some of the very low noise levels measured with the tunnel flowing. The noise floor with the tunnel flowing was not approached but the noise floor with both the tunnel flowing and the fan drive system fully loaded could not be established.

The spectral comparisons presented in figures 12-14 show that the suppressed noise levels with tunnel flow are in most instances as low or lower than those for the static tests. On the basis of this result, therefore, the noise performance of this fan with these suppressors in flight may be expected to be as good or better than that projected from conventional ground static test results.

The attenuation (difference in hardwall and treated inlet levels) obtained with the 3 inlets with and without tunnel flow are compared in figures 15-17. A distracting feature of the attenuation spectra is the region of negative attenuation at high frequencies. As will be discussed later, flow induced noise generated by perforated-plate/honeycomb configurations appears to be the cause of the negative attenuations. The treatment self-noise was judged to be confined to the highest 1/3-octave band shown in the spectra.

The attenuation spectra shown in figures 15-17 exhibit the varied behavior with inlet angle and fan speed that is typical of suppressor experiments. Any generalized attenuation properties that are observed, therefore, must often be qualified by the unique behavior observed at a particular angle or speed. Such deviations in consistency similarly limit any general assessment of the effect of tunnel flow on attenuation properties. Rather than using the specific comparisons shown in figures 15-17 to assess generalized effects, the comparison of average values shown in figures 18 and 19 will be used. The values displayed are the arithmetic averages of the attenuations at each frequency of the 6 spectra shown in the previous figures.

The average attenuation spectra for the three inlets are compared in figure 18 with and without tunnel flow and the spectra with and without tunnel flow are compared for each inlet in figure 19. The comparison of the inlets in figure 18 shows that the differences among attenuation spectra generally agree with the differences in design. Inlet B exhibits somewhat broader band attenuation than Inlet A and the attenuation of A(mod) is low at low frequencies because of the taping of the low frequency treatment section. The loss in attenuation for Inlet A(mod), due to taping, however, appears to occur at a somewhat lower frequency than that expected for its tuning frequency of 3550 Hz. The attenuations for Inlets A and A(mod) also do not exhibit the attenuation peak centering on 11,180 Hz as expected from the listed tuning frequency for the high frequency segment. The general observation is that the attenuation for all the honeycomb/perforate segments occurred at a lower frequency than that expected from the tuning frequency listed in Table II. The difference between the acoustic mode used for the design and the actual modal mixture experienced is a probable cause for such a shift in the frequency for maximum attenuation. The attenuation peak occurring at 6.3 kHz is at about the same level for all these inlets. The comparable levels at the mid frequency range were a design objective. In summary, the expected performance of the inlets relative to each other was obtained and the inlets can be considered representative state-of-the-art configurations.

The effect of tunnel flow on attenuation properties is best examined by referring to figure 19 where each inlet is considered separately. The effect of tunnel flow on attenuation primarily occurs in two frequency regions. One is centered near the BPF (about 2 kHz) and the other at about 6-7 kHz. At the BPF, the strong tone observed statically was reduced about 10 dB by tunnel flow and essentially eliminated. Inlet B responded strongly to this change in tone level. The attenuation near the BPF for Inlet B is very large without tunnel flow. With tunnel flow, the attenuation at the BPF is near that for the adjacent broadband frequency regions. This apparently enhanced attenuation of a strong tone has also been observed in other studies.[15] In this study, the strong BPF tone is caused by inflow disturbances and is not discrete. Whether the high attenuation is related to the modal mixtures of such inflow related tones and/or the response properties of the acoustic treatment is not known. Inlet A also exhibits some evidence of high tone attenuation whereas Inlet A(mod) appears to be insensitive to the disappearance of the BPF tone. The degree to which the BPF tone attenuation exceeds the broadband attenuation, therefore, appears to be directly related to the response of the treatment to broadband noise.

In the 6-7 kHz frequency region, some increase in attenuation due to tunnel flow is noted for all three inlets. Although the increase is small, Inlet A exhibits the largest increase and followed by Inlet A(mod) and B, respectively. This increase in attenuation occurs in the region of the BPF tone harmonics that were not designed to be cut-off. As discussed in the Section on source noise, rotor imperfections precluded the isolated appearance of tone harmonics with tunnel flow. The spectra with tunnel flow (fig. 8), however, did exhibit families of discrete shaft order tones in the 6-7 kHz region and figure 9 shows that tunnel flow increased the level of their tones. The modal properties associated with these shaft order tones could be a reason for increased attenuation. If it is, the honeycomb/

perforate treatment appears more responsive to the particular change in modal properties than the bulk absorber treatment of Inlet B.

In summary, these 1/3-octave band spectral comparisons show the attenuations by the inlets were as good or better with tunnel flow than without except for the high BPF tone attenuation obtained without tunnel flow.

Directivity Patterns

Figure 20 illustrates the on-line directivity patterns observed for Inlet B at the same conditions shown for the hardwall inlet in figure 6. These patterns are similar to those obtained with the other inlets and at other conditions. Figure 20, shows the time unsteadiness of the tones under static tests to be about the same level observed with the hardwall inlet. Time unsteadiness appears relatively insensitive to acoustic treatment. Tunnel flow, however, did reduce the time unsteadiness of the tones as was the case with the hardwall inlet.

The attenuation directivity patterns for Inlets A and B obtained from an analysis of the on-line records are shown for the 3 fan speeds in figures 21-23. Inlet A(mod) is not shown because of the malfunction of the boom microphone. One unusual feature of these directivity patterns is the oscillatory behavior with inlet angle exhibited at 2XBPF with tunnel flow. These variations are caused by changes in the lobular directivity pattern noted for the 2XBPF tone with tunnel flow. The acoustic modes responsible for the lobular patterns differed for the hardwall and treated inlets due to either some effect of the treatment on the inflow or due to an operating point change caused by the inlet pressure loss. The extreme sensitivity of the noise from this fan to a small change in operating condition was discussed previously. In either event, the varying behavior of the 2XBPF level cannot be considered an attenuation property of the acoustic treatment. The pattern includes the effects of a source noise change. An evaluation of the attenuation would require acoustic mode identification which is not possible at this time. The average attenuation over all inlet angles for the 2XBPF tone, however, does not appear to change significantly with tunnel flow for either inlet.

The attenuation patterns for the BPF shows a relatively smooth variation with inlet angle for both inlets. Without tunnel flow, the attenuation increases with an increase in inlet angle to a value often exceeding 10 dB. With tunnel flow, the attenuation is lower and tends to peak in the 60° to 80° angle region. At relatively large inlet angles, the attenuation is up to 10 dB lower with tunnel flow than without. These directivity patterns show that the high attenuation of the BPF under static tests, previously noted in the 1/3-octave spectra, maximized near the plane of the fan. This high attenuation at high inlet angles is expected from acoustic treatment. With tunnel flow, however, the BPF attenuation at high angles is low and decreasing. This difference in attenuation at high angles implies that tunnel flow not only reduced the BPF tone level but also reduced the proportion of modes near cut-off in the model mixture. The attenuation at 1.5XBPF at high inlet angles was also less with flow than without for the two lower fan speed conditions. This again implies that the source noise is less heavily weighted with modes near cut-off with tunnel flow than during static tests. The observation that tunnel flow decreased the relative number of modes near cut-off was also made in the previous Section on source noise characteristics.

The attenuation directivity at 2-1/2 BPF generally exhibits a maximum at 60° to 80° from the inlet both with and without tunnel flow. The maximum is usually somewhat higher with tunnel flow. The result implies that the acoustic treatment was most effective for the modes propagating to 60° to 80° although the reason for such selective attenuation was not apparent. In the source noise analysis, tunnel flow appeared to increase the proportion of modes propagating at 60° to 80° and reduce the proportion of modes near cut-off. This may account for the higher maximum attenuation and, in most instances, the loss in attenuation at high angles obtained with tunnel flow. The reason for the oscillatory behavior at high angles for the 2-1/2 BPF attenuation shown in figure 21 is not known.

In summary, the effects of tunnel flow on attenuation with Inlets A and B are primarily related to the flow effects on fan source noise noted previously. Both inlets appear to predictably respond to changes in the modal mixtures of the source noise. The population density of the modes in the mixture expressed in terms of cut-off or propagation angle appears to be the major variable affecting attenuation properties.

Narrowband Spectra

Typical narrowband spectra for the fan operating with Inlets A and B obtained statically and with tunnel flow are shown in figure 24. The operating condition for these spectra is the same as for the hardwall inlet spectra shown in figure 8. In general appearance, the changes in the spectra due to tunnel flow for the treated inlet are much the same as that observed with the hardwall inlet. Tunnel flow decreased the BPF tone and exposed a multiplicity of highly variable shaft order tones. As concluded previously, a rotor with undefined imperfections is responsible for the shaft order tone content in the spectra.

The attenuations inferred by these narrowband spectra are shown in figures 25 and 26 where the differences between the hardwall and treated inlet spectra are presented. These attenuations are mainly instructive to show that spectral differences obtained with tunnel flow exhibit larger variations with frequency than those for the static tests. A detailed discussion of the attenuation of specific shaft order tones is not considered useful for two reasons. One is that the attenuations vary significantly with inlet angle in some unknown manner. The other is related to the previously discussed sensitivity of the shaft order tone content of the spectra to a small change in operating condition. It is possible that the pressure loss of the treated inlets caused a small change in operating condition. The difference in the hardwall and treated inlet spectra, therefore, contain a combination of source noise changes and attenuation properties. Such spectral changes are important to the spectral detail of attenuation obtained from narrowband analysis but have little impact on the 1/3-octave band analysis previously discussed. The attenuation spectra shown in figures 24-26, however, reveal the

spectral structures that can exist within a 1/3-octave band and suggests that the 1/3-octave band notions of broadband and BPF tone noise used previously cannot be considered too literally.

Comparison with Previous Results

The tests of the treated inlets with and without tunnel flow showed a variation in attenuation properties dependent on source noise characteristics. A change in fan configuration with its differing source noise would also be expected to affect attenuation properties. This is confirmed by a comparison of Inlets A and B results using Rotor-55 with those obtained statically using the QCSEE-simulator fan.[6] The QCSEE-simulator is a somewhat higher tip speed fan with more rotor blades and without BPF tone cut-off at the design speed.

Typical 1/3-octave band spectra for the hardwall and treated inlets obtained with the QCSEE-Simulator fan and the NASA fan in static tests can be compared in figure 27. The data shown for the two fans are for comparable fan total pressure rises. The spectral shapes are similar for the two fans, however, the BPF is at a higher frequency for the QCSEE fan. Spectral differences between the two fans primarily occur at frequencies below the BPF. In this region the level for the hardwall inlet and the attenuation obtained from Inlets A and B are higher with the QCSEE fan than with the Rotor-55 fan. The narrowband spectra for the hardwall QCSEE configuration at the operating condition for figure 27 is shown in figure 28. Shaft order tones exist throughout the spectra but at frequencies below the BPF these tones are much more pronounced than those observed for the NASA fan in figure 8. These lower frequency tones may signal the approach of sonic tip speed conditions where such tones are usually caused by shock structures attached to the blades. At 90% of design fan speed, however, the relative tip Mach number is only about 0.85 and a shock structure would not normally exist. The prevalence of shaft order tones in figure 28, therefore, may simply be indicative of rotor imperfections as in the case of the NASA fan. Regardless of the source of these tones, the source noise for the QCSEE fan at low frequencies consists of relatively strong shaft order tones.

The directivities of the attenuation obtained from Inlets A and B with the QCSEE fan at 90% speed are shown in figure 29. These directivities are from reported 1/3-octave band spectra taken at 10° increments in the inlet quadrant. Directivities are shown for 1/3-octave frequencies comparable to those used in the NASA tests except that the behavior at two lower frequencies is also displayed. In general, attenuation increased with inlet angle. This behavior, as previously discussed, is indicative of both a source noise mode mixture weighted toward cut-off modes and a preference of acoustic treatment to attenuate modes near cut-off. The attenuation at 0.5 BPF is an exception. At this frequency a relatively high attenuation is exhibited at all angles including the fan axis. The inlets, therefore, were very effective in reducing the level of the strong shaft order tones observed in this frequency region. The high attenuation along the fan axis is not expected from acoustic treatment and the attenuation levels at 0.5 BPF, therefore, are suspected to contain some combination of attenuation and either a change in source noise or manner of duct propagation.

The source noise characteristics and the inlet attenuation varied with fan speed in the QCSEE tests as was the case in the NASA tests. In particular, the QCSEE tests included the changes in fan source noise encountered during the transition to supersonic tip speed operation. Neglecting these differences, a comparison of the average attenuations obtained with the QCSEE fan with those for the NASA fan is shown in figure 30. The average at 60° and 90° at all test conditions for the QCSEE fan are compared with similar averages for the NASA fan previously shown in figure 19. The differences in the attenuation spectra appear most pronounced at frequencies less than about 6 kHz for both Inlets A and B. The QCSEE results show better agreement with the NASA static test results than with the NASA tunnel flow tests. In general, however, the average attenuation below 6 kHz was greatest for the static QCSEE tests. The low frequency peak for the Inlet B in the NASA static tests probably should be neglected in this generality. This peak closely approximates the BPF tone suppression, whereas, in the QCSEE tests any optimum BPF tone properties are obscured by averaging over a large speed change. Also a prominent BPF tone was not present at supersonic tip speeds in the QCSEE tests.

The conclusion drawn from comparisons with the QCSEE results is that attenuation below about 6 kHz is highly sensitive to the source noise present (with Inlet B appearing more sensitive than Inlet A). Attenuation at low frequencies appears to be high because strong shaft order tones are present and the behavior is similar to the high BPF tone attenuation experienced in the NASA static tests.

Treatment Self-Noise

The negative attenuation at 20 kHz noted earlier for Inlets A and A(mod) in the NASA tests was also evident in the QCSEE test results. The negative attenuations were observed at nearly all inlet angles and test conditions and resulted in the average negative attenuation shown in figure 30. Noise generated by the acoustic treatment is a probable cause for the negative attenuations. This additional noise for Inlet A is evident in the spectra shown in figure 27. A peak that protrudes above the hardwall inlet level at 20 kHz is evident for the QCSEE results and a peak is also implied in the NASA results.

Flow through a duct line with honeycomb/perforate treatment can generate a tone-like noise. Recent investigators[16,17] of this treatment self-noise have concluded that the noise is generated when the airjets formed by the activated acoustic treatment are exposed to a cross-flow. A tone-like noise completely contained within a 1/3-octave bandwidth is usually generated. The frequency of this noise corresponds to the vortex shedding frequency for flow past cylinders with diameters equal to the hole size in the perforated faceplate. The jetting action of the treatment occurs when honeycomb/perforate structure is exposed to the pressure disturbances in the turbulent boundary layer or to acoustic pressures. The jetting action always exists but is strongest when the frequency range of the exciting disturbances encompass the tuning frequency of the treatment. Jetting action is not expected or is highly subdued with the bulk-absorber/perforate treatment.

The predicted frequency for the treatment self-noise is obtained from the Strouhal number relationship given by

$$S = \frac{fD}{v}$$

when S is the Strouhal number, f is the frequency of the generated noise, D is the hole diameter in the face plate and v is the crossflow or duct velocity. The Strouhal number has been found to be relatively constant although there is some dependence on hole diameter and velocity. For the conditions of the fan tests, the Strouhal number is about 0.2.

The duct Mach number in the fan tests was a variable because of changes in fan speed and diffusion in the inlet. Typically, the Mach number was about 0.6 or a velocity of about 174 m/sec. The hole diameter for Inlet A is 0.158 cm. Using these values, the predicted frequency is 22 kHz. A tone-like noise at this frequency would fall in the 20 kHz 1/3-octave band. The result implies that treatment self-noise was the source of the addition noise and the cause of the apparent negative attenuations at the 20 kHz 1/3-octave band frequency for Inlet A as well as Inlet A(mod).

The sound power level in the 20 kHz 1/3-octave band reported for the QCSEE tests translates into an intensity level of about 125 dB in the duct. The NASA data have a similar duct intensity level. Measurements of duct intensities in experiments with treatment self-noise[16,17] show the intensity to be highly variable. Measured levels for various configurations ranges from 110 to 150 dB. A level of 125 dB, as inferred from the fan tests, is in this range and also tends to identify the additional noise as treatment self-noise.

Summary of Results

The results of the tests made to evaluate the effect of inflow clean-up obtained by wind tunnel flow on the attenuation properties of three treated low-Mach-number inlets using a subsonic tip speed fan are summarized as follows.

1. The far field noise levels of the fan stage with the treated inlets measured under conditions of simulated flight were generally as low or lower than those obtained under static test conditions.

2. Tunnel flow significantly affected the fan source noise and thus the attenuation by the treated inlets. Alterations in the attenuation were mostly confined to the frequency region where source noise changes were observed. The effects observed in 1/3-octave-band analyses of fixed and traversing microphone measurements are summarized in results 3 to 7.

3. The source noise is characterized by a strong blade passage frequency (BPF) tone in static test but not with the tunnel flowing because of the cut-off design features of the fan stage. In static tests, the strong tone was more highly attenuated than the adjacent broadband noise. The difference in attenuation varied with the response of the inlet treatment and in some instances approached 10 dB. With tunnel flow, when tone cut-off was observed, the attenuation at the tone frequency was comparable to that for broadband noise. Directivity results for the BPF imply that tunnel flow reduces the proportion of modes near cut-off.

4. The design intent of the inlets was qualitatively exhibited in both a static and tunnel flow comparison of averaged attenuation properties. The static results, however, exhibit the high attenuation of the BPF tone that varies with the response properties of the inlet. The maximum attenuation at mid-frequencies expected in the attenuation spectra was observed. The maximum was larger by several dB in the tunnel flowing tests. The maximum, however, appeared to occur at a frequency of about one-half that expected from the reported tuning frequency of the treatment. The modal content of the noise that controls the frequency of the peak attenuation for the treatment apparently differed significantly from the single mode assumption used for the calculated values.

5. The attenuation directivity of the 2XBPF tone with tunnel flow was highly variable compared to that obtained statically. The variable attenuation was caused by the lobular directivity pattern that characterized the 2XBPF tone during tunnel flow. The treated inlets altered the shape of the lobular directivity pattern and the implied attenuation directivity is a combination of both attenuation and source noise changes. The average attenuation over the far field, however, was not significantly affected by tunnel flow.

6. Attenuation directivity at 1-1/2XBPF, presumed to be broadband noise, generally exhibited a loss in attenuation at high directivity angles due to tunnel flow. Source noise also was reduced by tunnel flow at high angles. The results imply that tunnel flow causes a relative decrease in the propagation energy of the modes near cut-off.

7. Attenuation directivity at 2-1/2XBPF, presumed to be broadband noise, exhibited a maximum in the region 60° to 80° from the inlet axis. This maximum attenuation was usually increased by tunnel flow and the increase appears to relate to an increase in source noise propagating in the 60° to 80° direction.

8. Narrowband spectral analyses revealed that fan source noise is characterized by a multiplicity of shaft order tones that is indicative of unequal rotor blade spacings or angle settings. The 1/3-octave bands, particularly with tunnel flow, do not, therefore, simply contain a dominant BPF tone and/or broadband noise but can also include relatively prominent shaft order tones. The level and number of these tones are highly variable with inlet angle and with changes in fan speed and inlet configuration. These shaft order tone properties preclude the use of the relatively simple modal characterization of the BPF tones that is based on perfect fan stage geometry. The modal description at all frequencies appears to be highly complex.

9. A comparison of the attenuation results with those from previous static tests of the inlets with a different fan stage shows qualitative agreement. The difference in attenuation was comparable in magnitude to that noted between static and tunnel flow tests with the same fan and can be identified with source noise changes.

10. A tone-like treatment self-noise at a frequency of 20 kHz was identified in the results

obtained with inlets using a honeycomb/perforate treatment. The self-noise accounted for the implied values of negative attenuation observed at 20 kHz.

References

1. Merriman, J. E. and Good, R. C., "Effect of Forward Motion on Fan Noise," AIAA Paper 75-464, Hampton, Va., 1975.

2. Rice, E. J., "Spinning Mode Sound Propagation in Ducts with Acoustic Treatment," NASA TN D-7913, 1975.

3. Heidmann, M. F. and Dietrich, D. A., "Simulation of Flight-Type Engine Fan Noise in the NASA-Lewis 9x15 Anechoic Wind Tunnel," NASA TM X-73540, 1977.

4. Dietrich, D. A., Heidmann, M. F., and Abbott, J. M., "Acoustic Signatures of a Model Fan in the NASA-Lewis Anechoic Wind Tunnel," AIAA Paper 77-59, Los Angeles, Calif., 1977.

5. Tyler, J. M. and Sofrin, T. G., "Axial Flow Compressor Noise Studies," SAE Transactions, Vol. 70, 1962, pp. 309-332.

6. Bilwakesh, K. R. and Clemons, A., "Acoustic Tests on a 20-Inch Diameter Scale Model Fan and Inlet for the Under-the-Wing Engine (QCSEE)," General Electric Co., CR-135117, 1975.

7. Abbott, J. M., Dietrich, J. H., and Williams, R. C., "Low Speed Aerodynamic Performance of 50.8 cm Diameter Noise Suppressing Inlets for the Quiet, Clean, Short-Haul Experimental Engine (QCSEE)," NASA TM to be published.

8. Mather, J. S. B., Savidge, J., and Fisher, M. J., "New Observations on Tone Generation in Fans," Journal of Sound and Vibration, Vol. 16, 1971, pp. 407-418.

9. Mugridge, B. D., "Axial Flow Fan Noise Caused by Inlet Flow Distortions," Journal of Sound and Vibration, Vol. 40, 1975, pp. 497-512.

10. Duncan, P. E. and Dawson, B., "Reduction of Interaction Tones From Axial Flow Fans by Non-Uniform Distribution of the Stator Vanes," Journal of Sound and Vibration, Vol. 38, 1975, pp. 357-371.

11. Saule, A. V., "Some Observations About the Components of Transonic Fan Noise from Narrow-Band Spectral Analysis," NASA TN D-7788, 1974.

12. Saule, A. V., "Modal Structure Inferred From Static Far-Field Noise Directivity," AIAA Paper 76-574, Palo Alto, Calif., 1976.

13. Rice, E. J., "Multimodal Far-Field Acoustic Radiation Pattern - An Approximate Equation," AIAA Paper 77-1281, Oct. 1977.

14. Rice, E. J., "Inlet Noise Suppressor Design Method Based Upon the Distribution of Acoustic Power with Mode Cutoff Ratio," in Advances in Engineering Science, NASA CP-2001-Vol. 3, 1977, pp. 883-894.

15. Aircraft Engine Noise Reduction, NASA SP-311, 2972.

16. Tsui, C. Y. and Flandro, G. A., "Self-Induced Sound Generation by Flow Over Perforated Duct Liners," Journal of Sound and Vibration, Vol. 50, 1977, pp. 315-331.

17. Bauer, A. B. and Chapkis, R. L., "Noise Generated by Boundary-Layer Interaction with Perforated Acoustic Liners," Journal of Aircraft, Vol. 14, Feb. 1977, pp. 157-166.

TABLE I. - FAN DESIGN PARAMETERS

Fan diameter	20 in. (50.8 cm)
Pressure ratio	1.2
Rotor tip speed	700 ft/sec (213 m/s)
Hub/tip ratio	0.46
Rotor tip solidity	0.9
Rotor/stator spacing	1 chord (nominal)
Rotor blades	15
Stator vanes	25
Vane/blade ratio	1.67

E-9247

TABLE II. - INLET DESIGNS

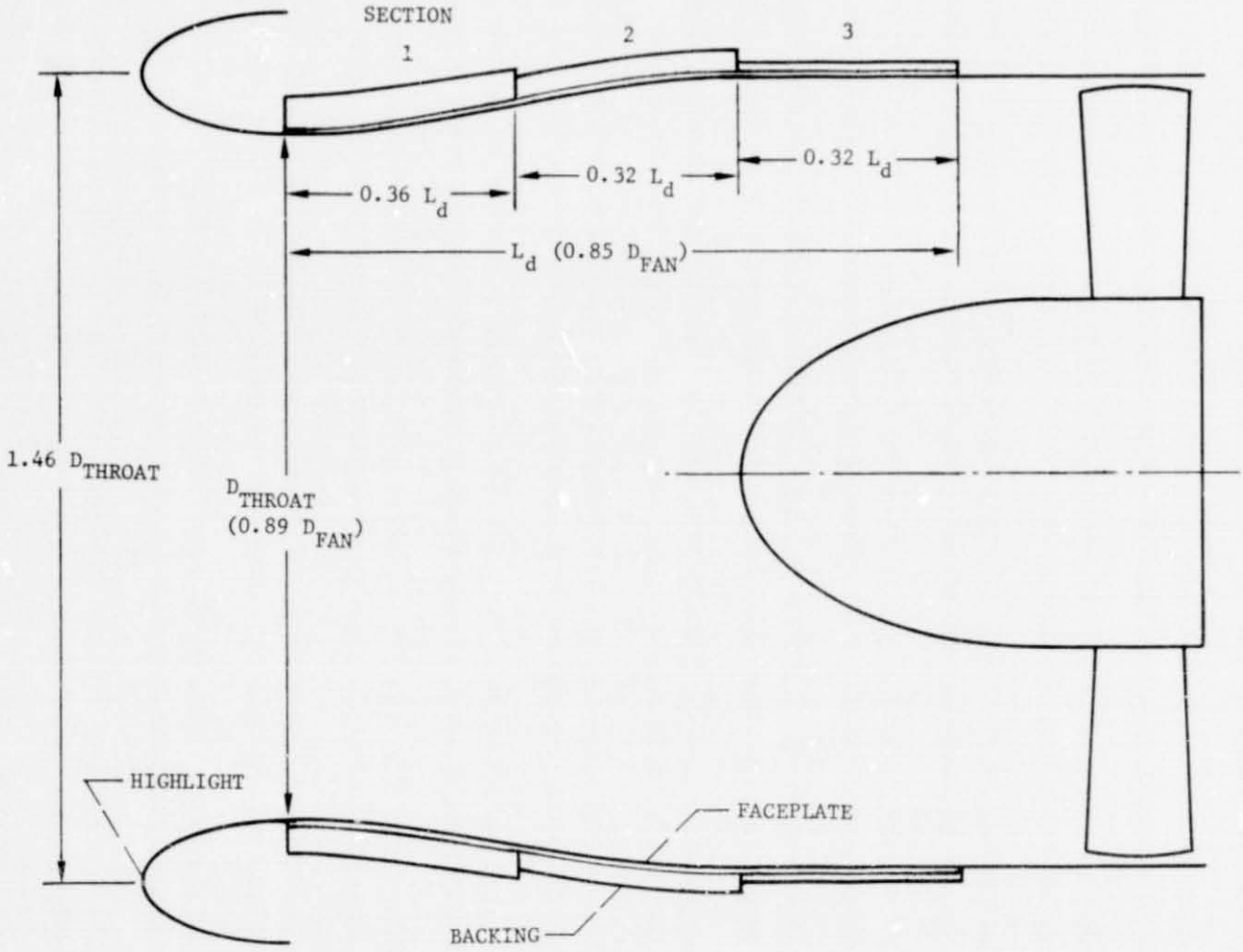

Inlets	Section	Tuning frequency calculation, Hz	Perforated faceplate			Backing	
			Porosity, percent	Hole diameter, cm	Thickness, cm	Depth, cm	Material
A	1	3 550	10	0.158	0.0508	1.42	Honeycomb
	2	7 100	10	.158	.0508	.325	Honeycomb
	3	11 180	10	.158	.0508	.134	Honeycomb
A(mod)	1	------	Taped	-----	------	-----	----------
	2	7 100	10	0.158	0.0508	0.325	Honeycomb
	3	11 100	10	.158	.0508	.134	Honeycomb
B	1	Broadband properties	28	0.114	0.081	1.27	Bulk absorber (Scottfelt)
	2		28	.114	.081	1.27	Bulk absorber (Scottfelt)
	3		28	.114	.081	1.27	Bulk absorber (Scottfelt)
Hardwall	Solid faceplate, all sections						

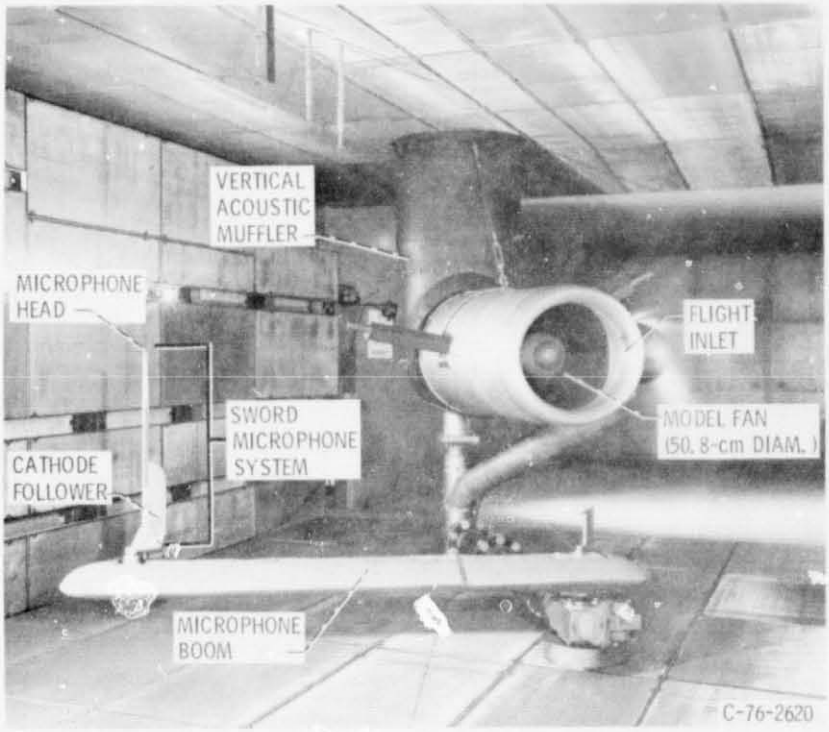

Figure 1. - Model fan installed in the anechoic wind tunnel.

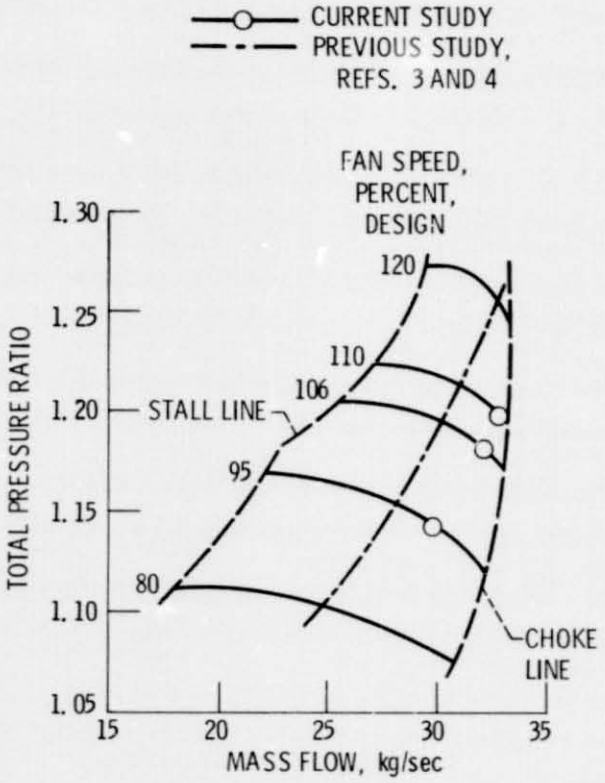

Figure 2. - Performance map of model fan.

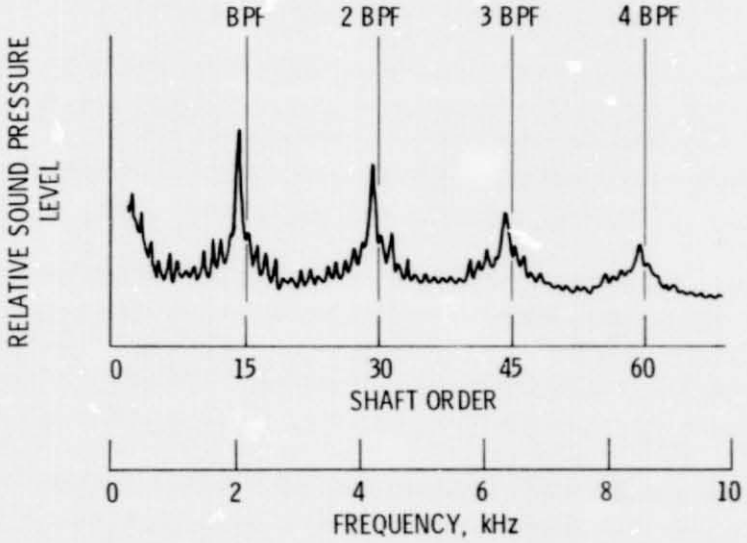

Figure 3. - Typical narrowband spectra for static test conditions showing shaft order tones.

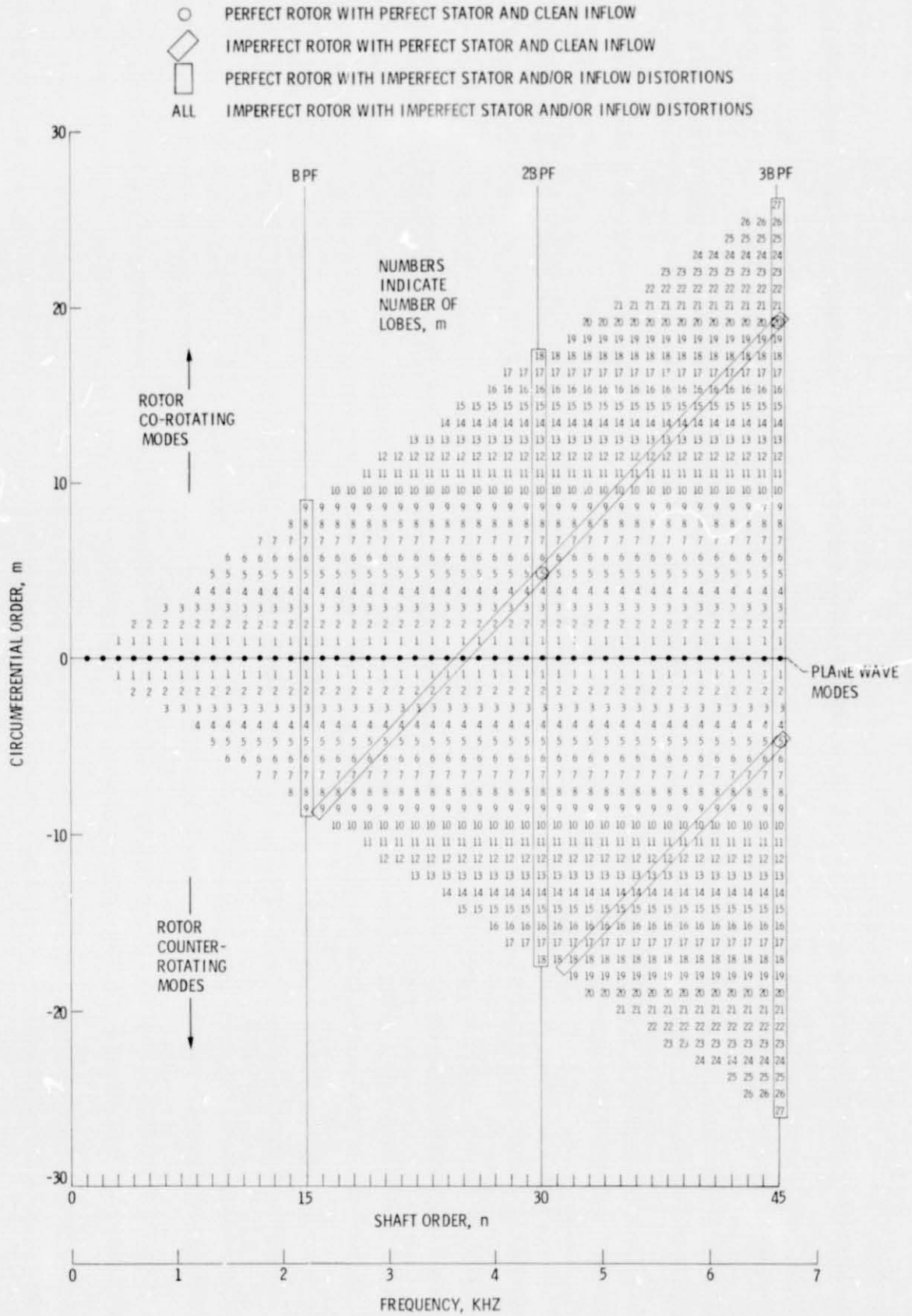

Figure 4. - Allowable lowest radial order spinning acoustic modes for model fan at 106% design speed.

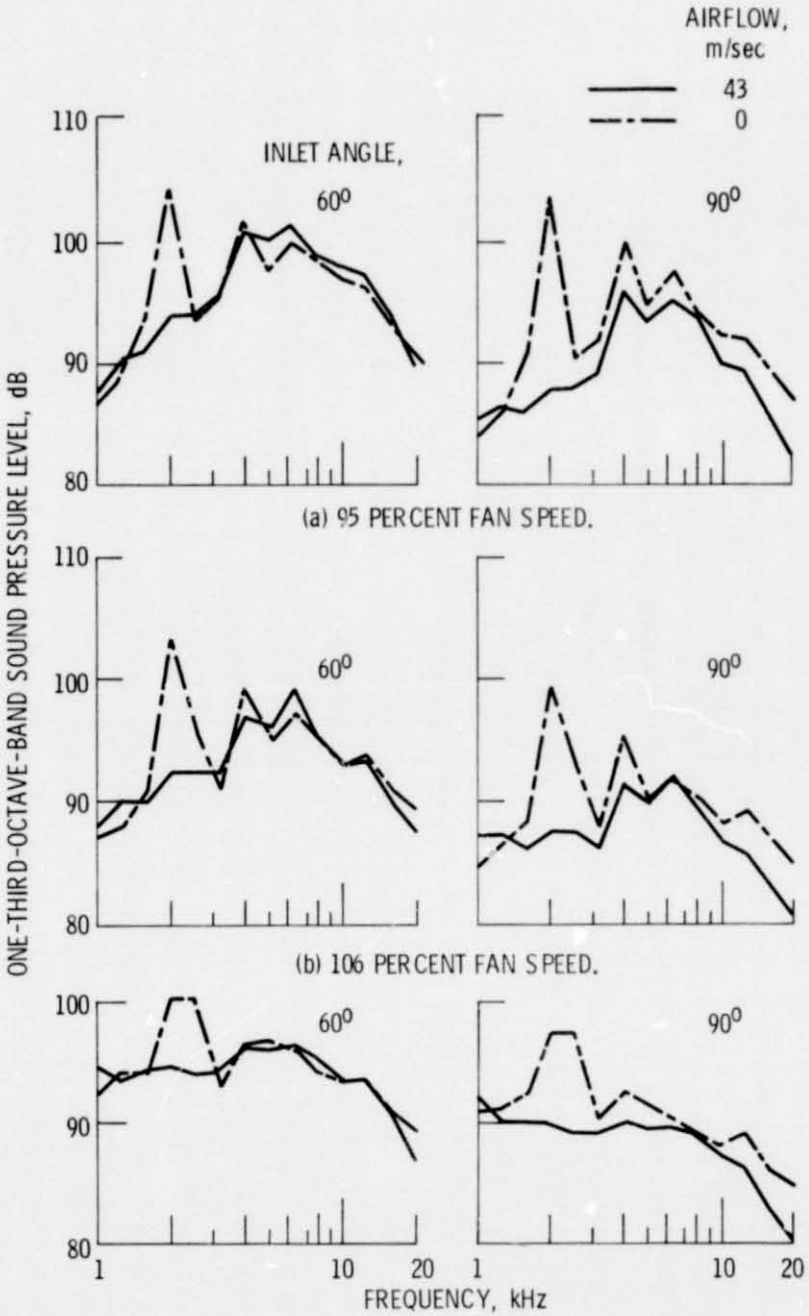

Figure 7. - Hardwall inlet far-field spectral properties.

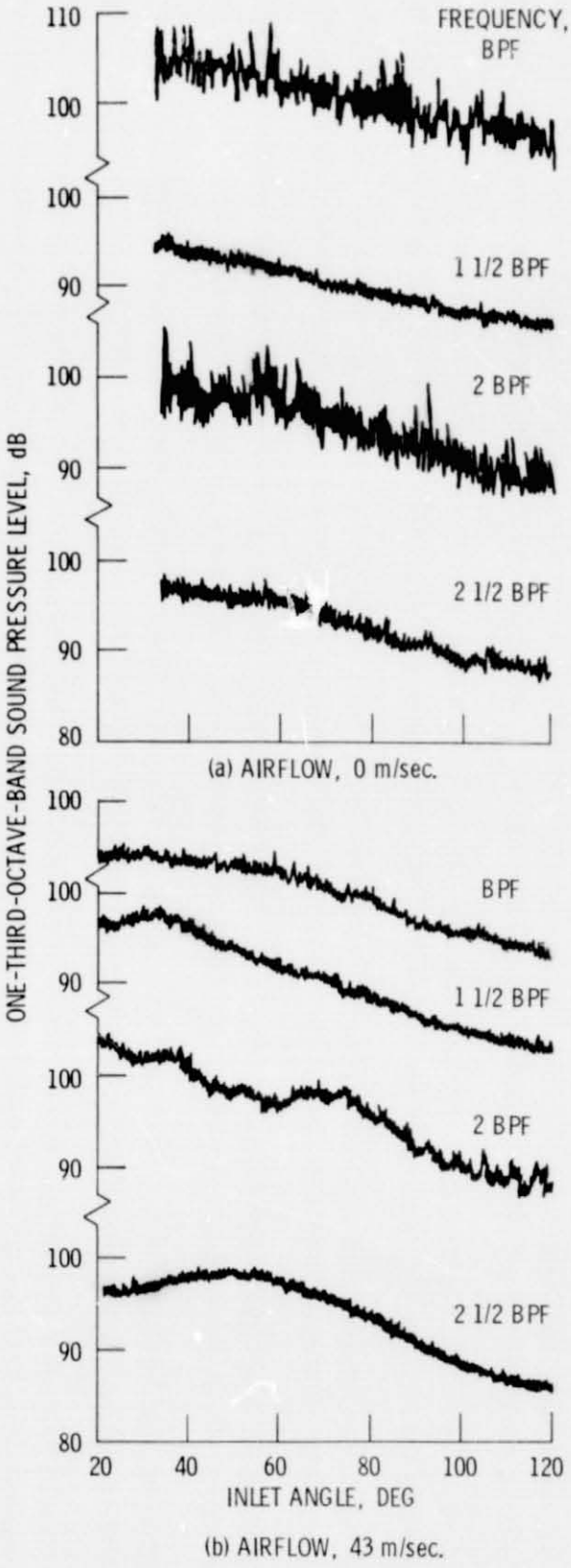

Figure 6. - Hardwall inlet directivity patterns at 106 percent fan speed.

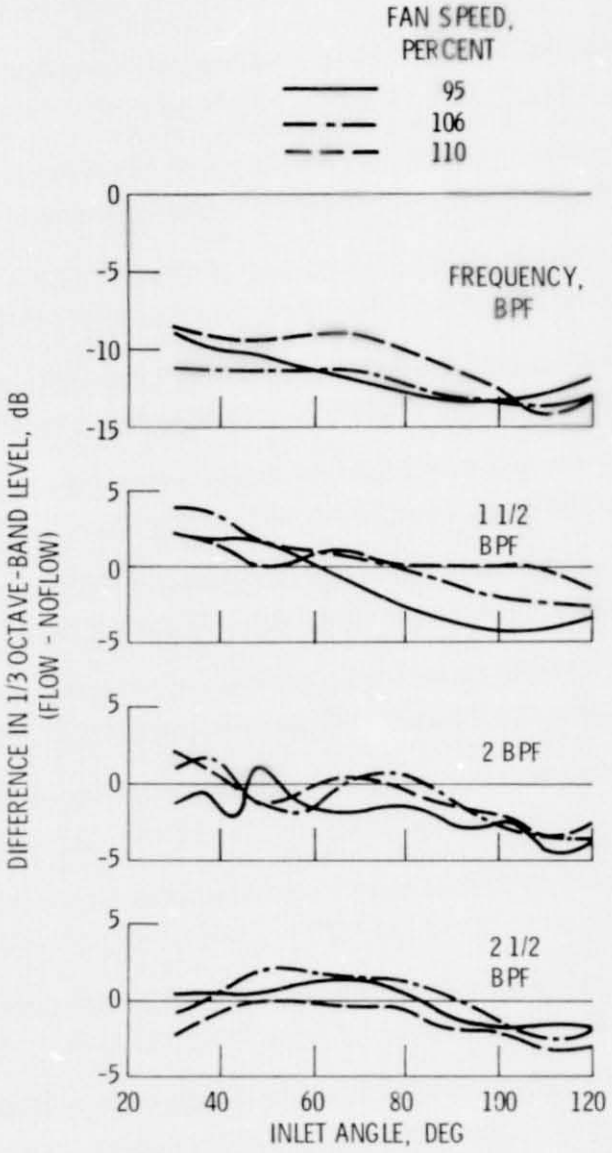

Figure 7. - Effect of tunnel flow on directivity patterns of hardwall inlet.

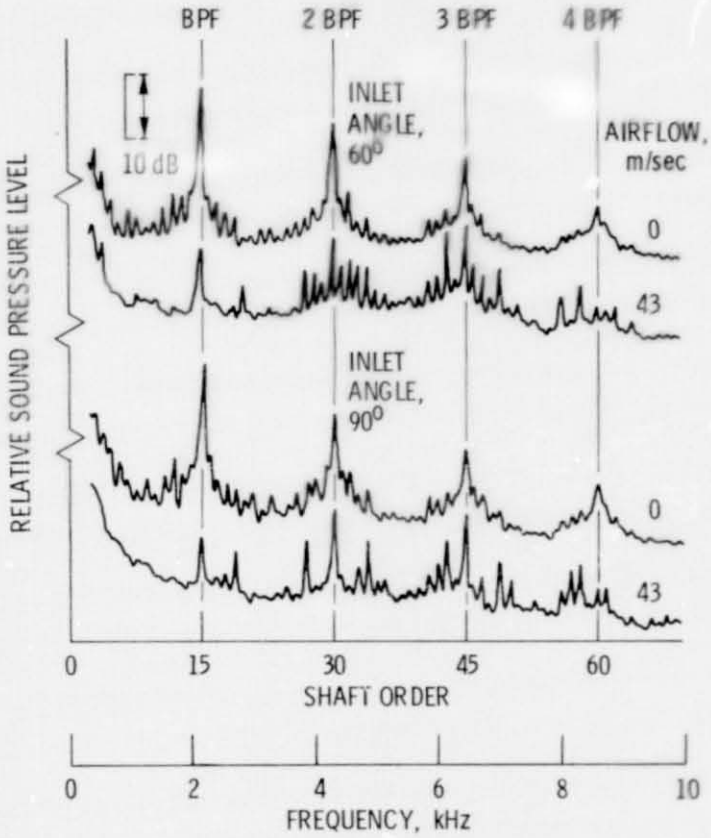

Figure 8. - Hardwall inlet narrowband spectra at 106 percent fan speed.

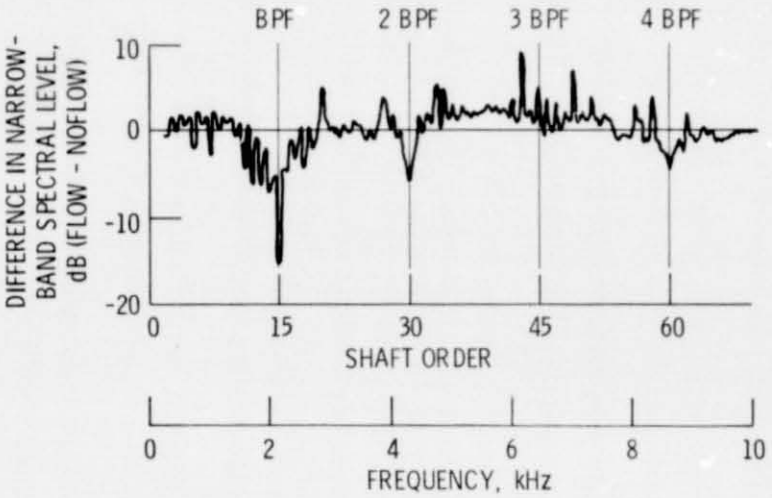

Figure 9. - Difference in narrowband spectral levels at 60^0 caused by wind tunnel airflow.

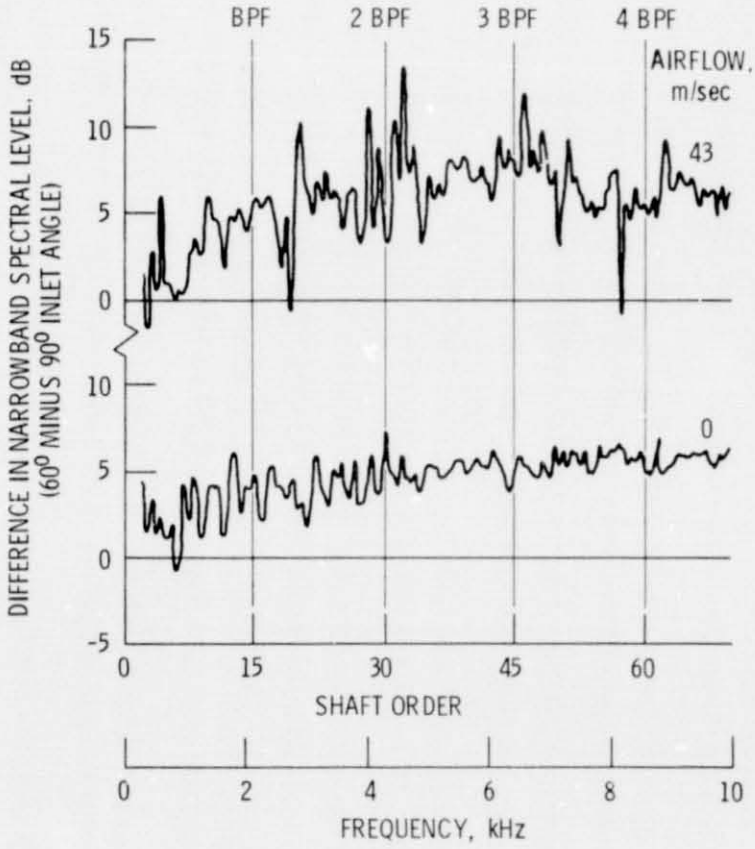

Figure 10. - Difference in narrowband spectral levels measured at inlet angles of 60^0 and 90^0.

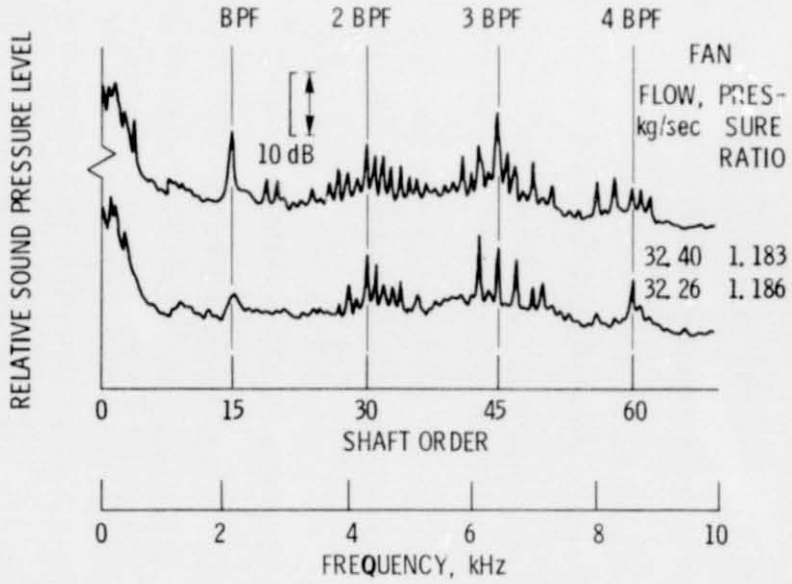

(a) NARROWBAND SPECTRA.

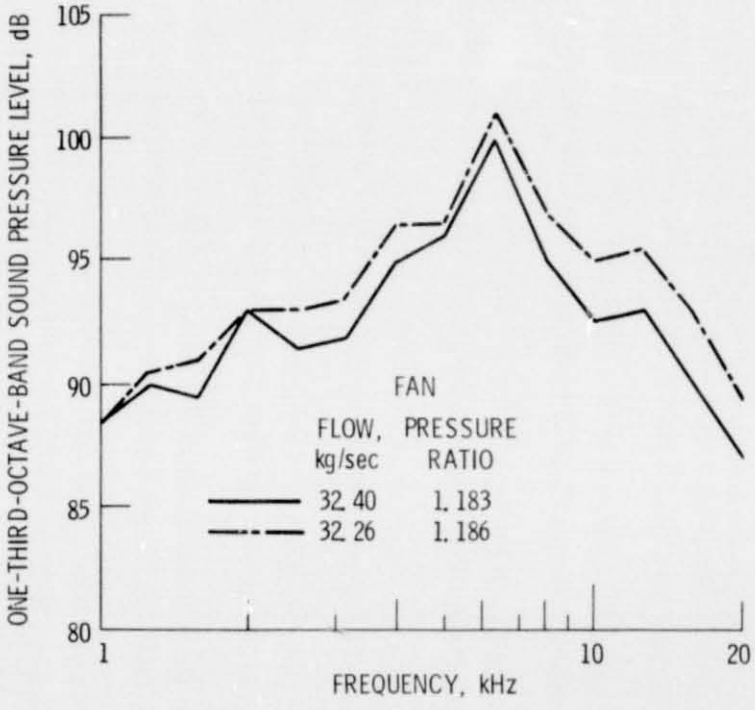

(b) ONE-THIRD-OCTAVE-BAND SPECTRA.

Figure 11. - Effect of small fan operating line change on spectra properties at 106 percent fan speed and 60^0 inlet angle.

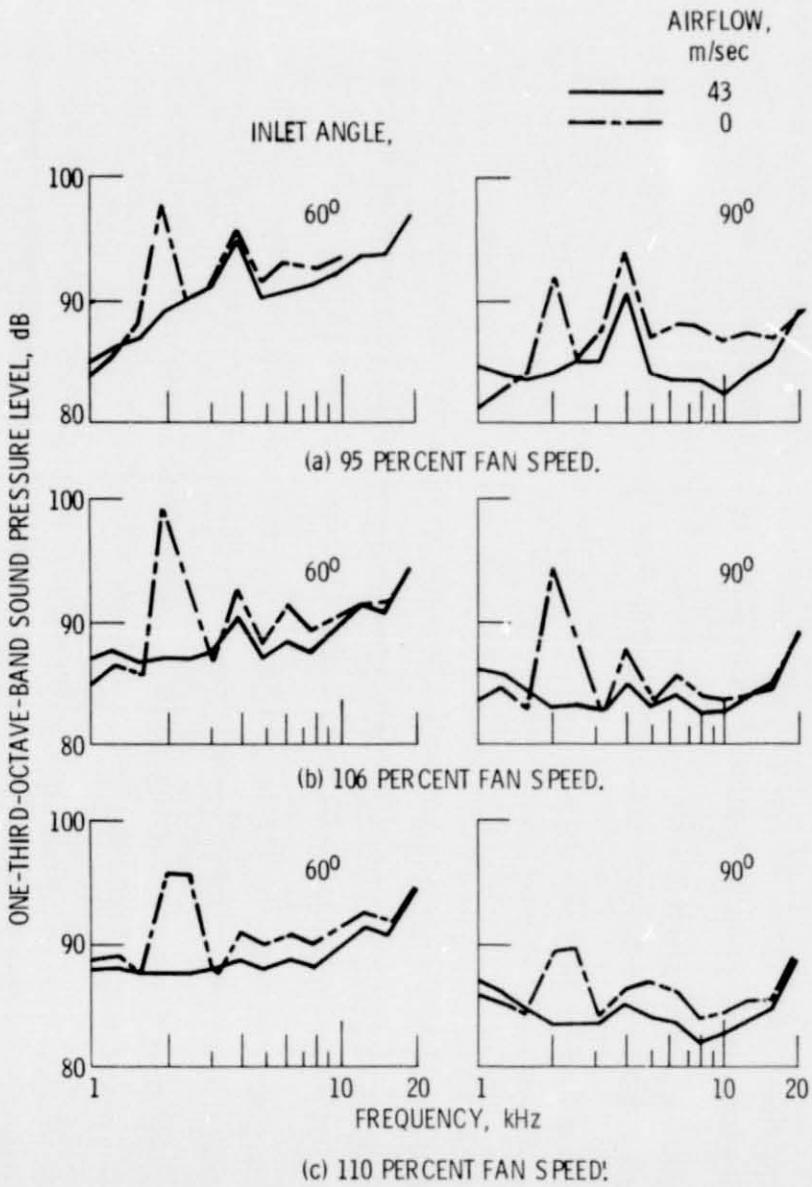

Figure 12. - Inlet A (3 segment honeycomb) far-field spectral properties.

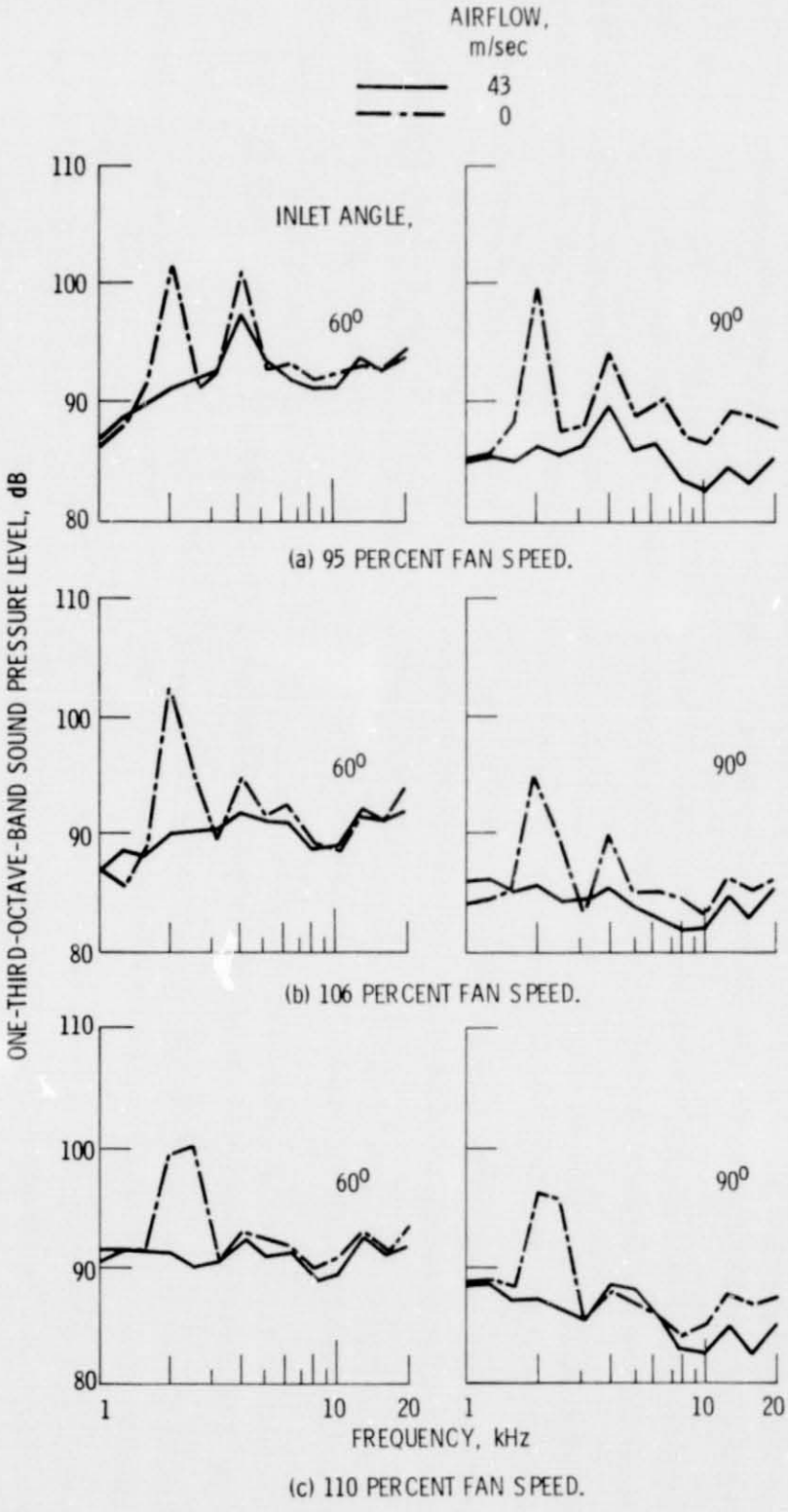

Figure 13. - Inlet A(MOD) (2 segment honeycomb) far-field spectral properties.

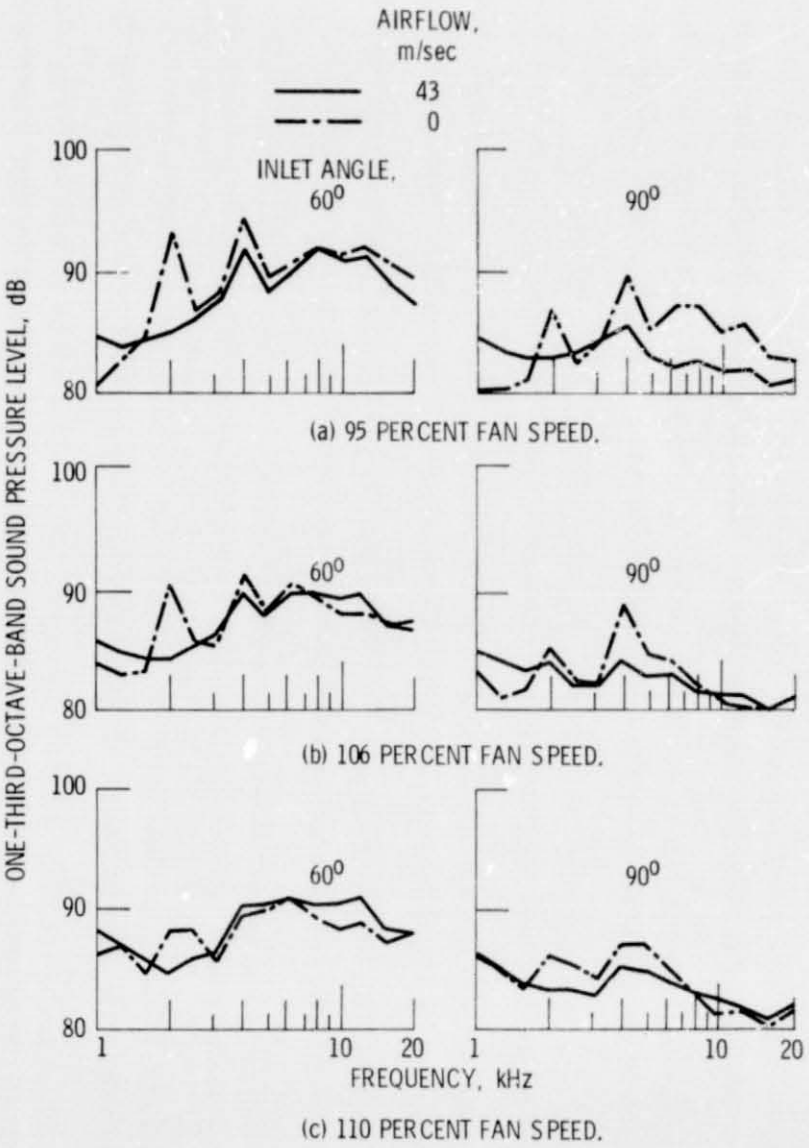

Figure 14. - Inlet B (bulk absorber) far-field spectral properties.

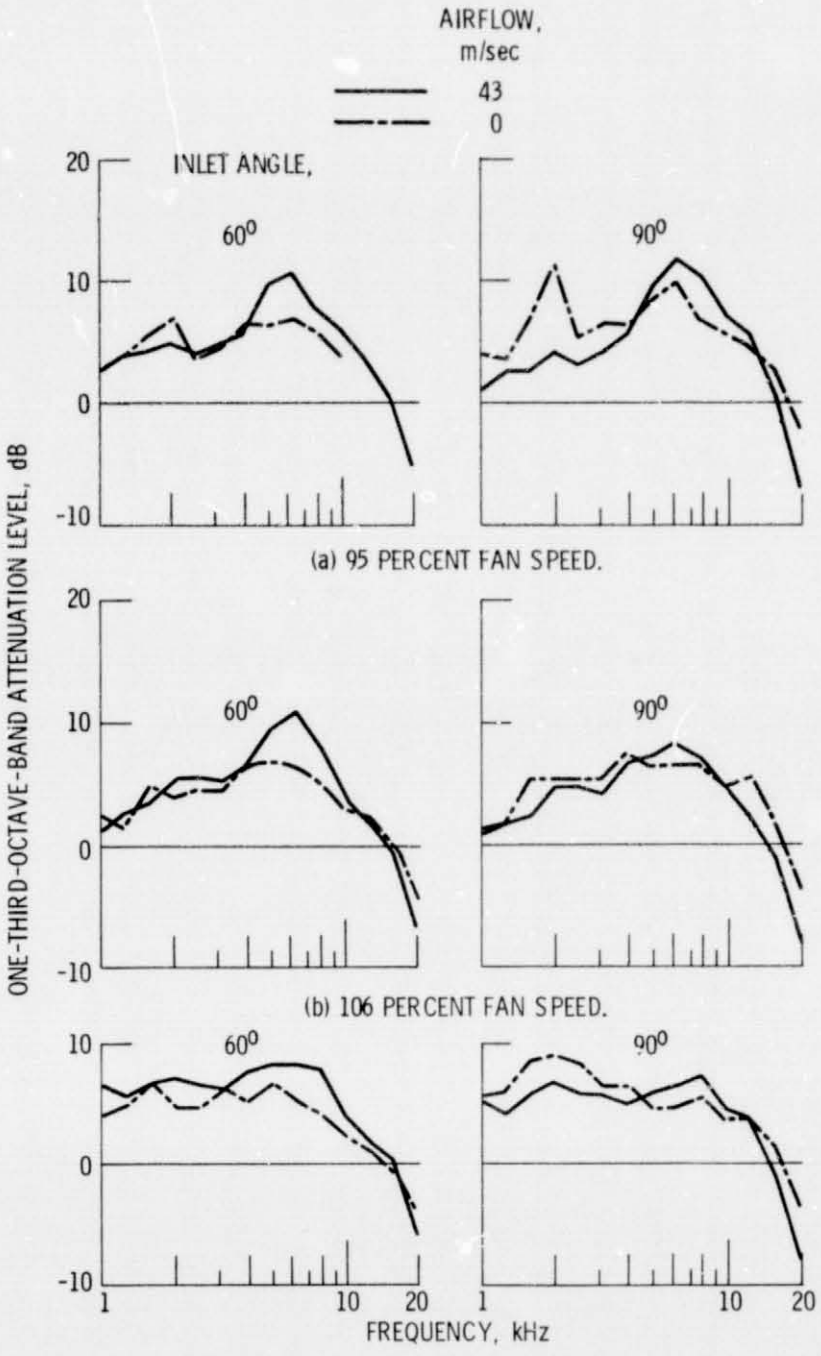

Figure 15. - Inlet A (3 segment honeycomb) attenuation spectra.

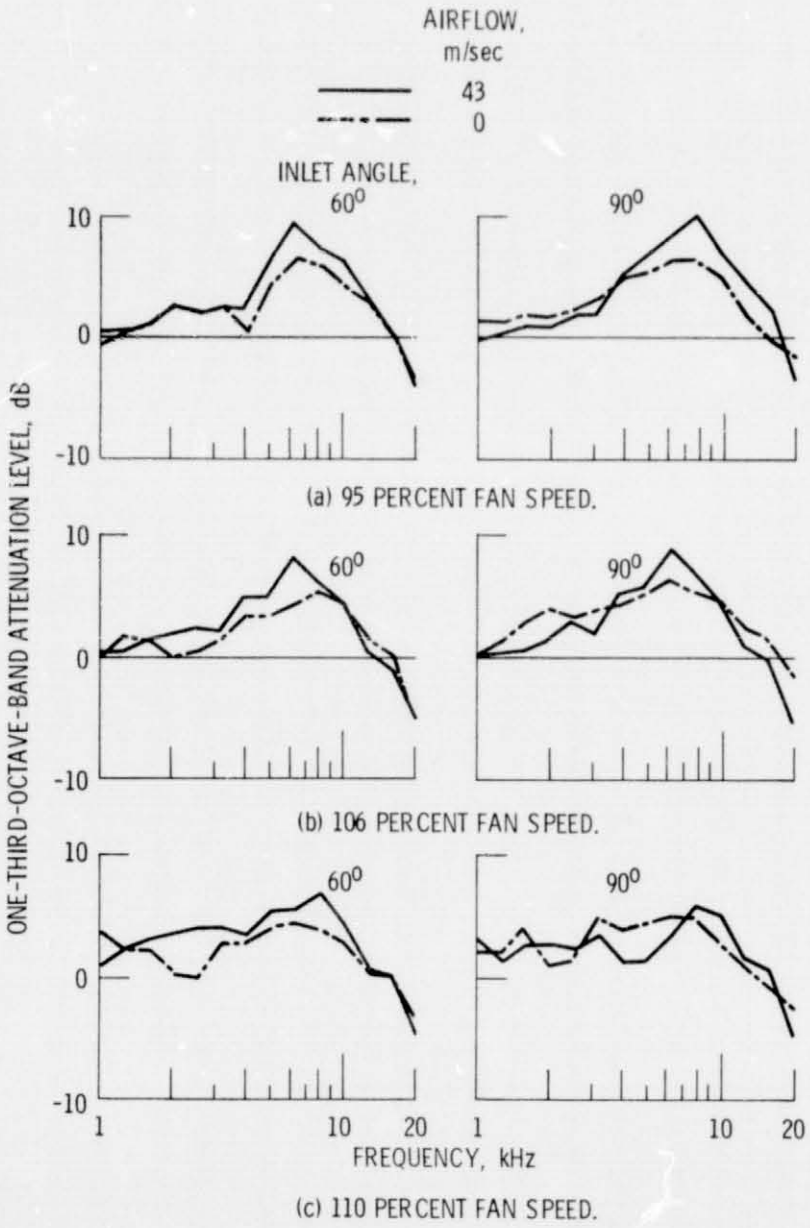

Figure 16. - Inlet A(MOD) (2 segment honeycomb) attenuation spectra.

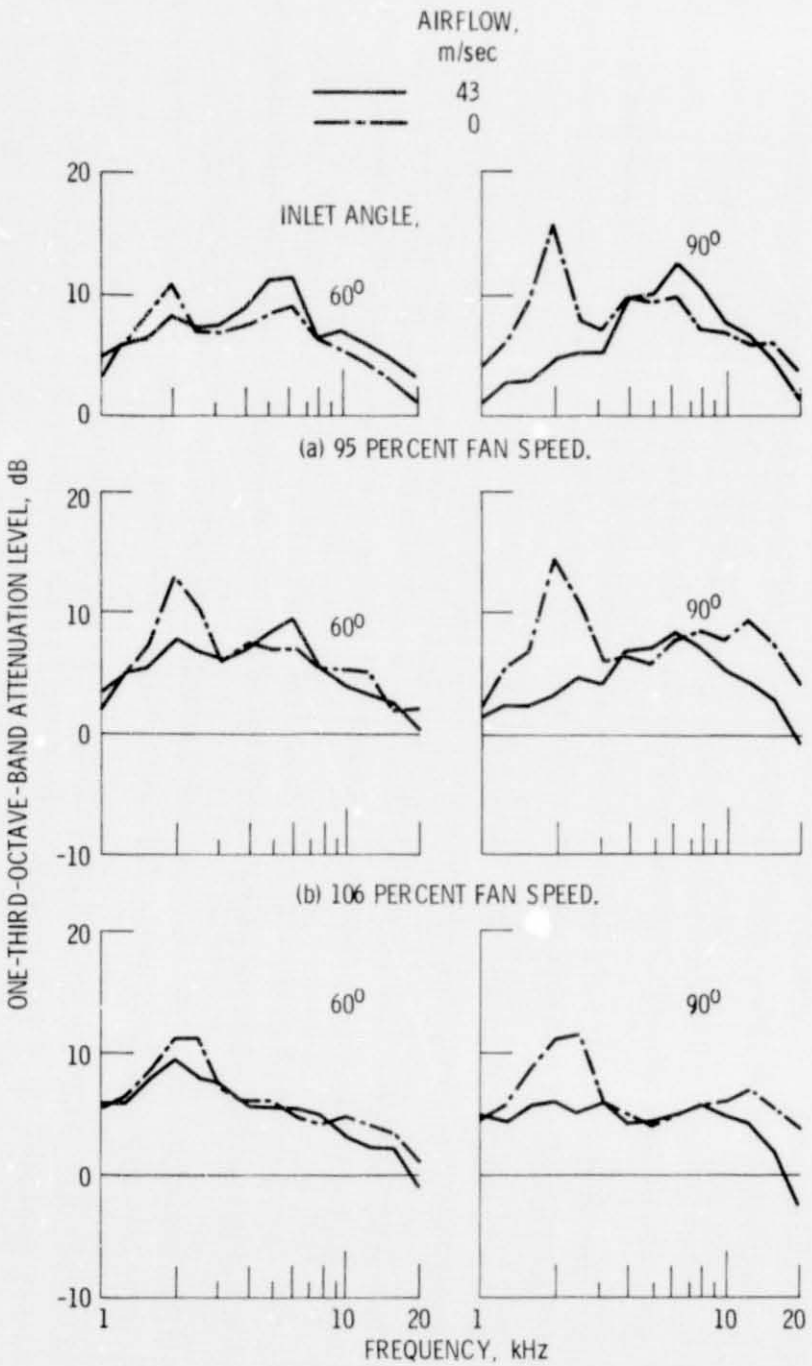

(a) 95 PERCENT FAN SPEED.

(b) 106 PERCENT FAN SPEED.

(c) 110 PERCENT FAN SPEED.

Figure 17. - Inlet B (bulk absorber) attenuation spectra.

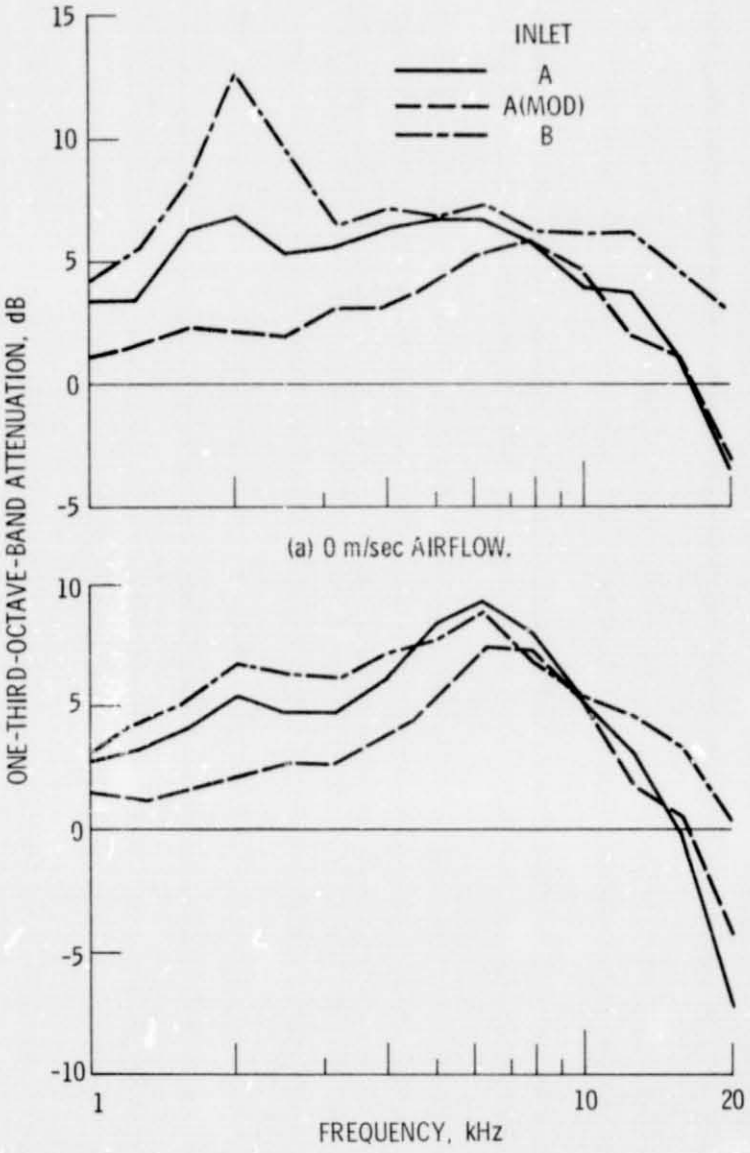

Figure 18. - Comparison of attenuation levels averaged over 95, 106, and 110 percent fan speeds and 60^0 and 90^0 inlet angles.

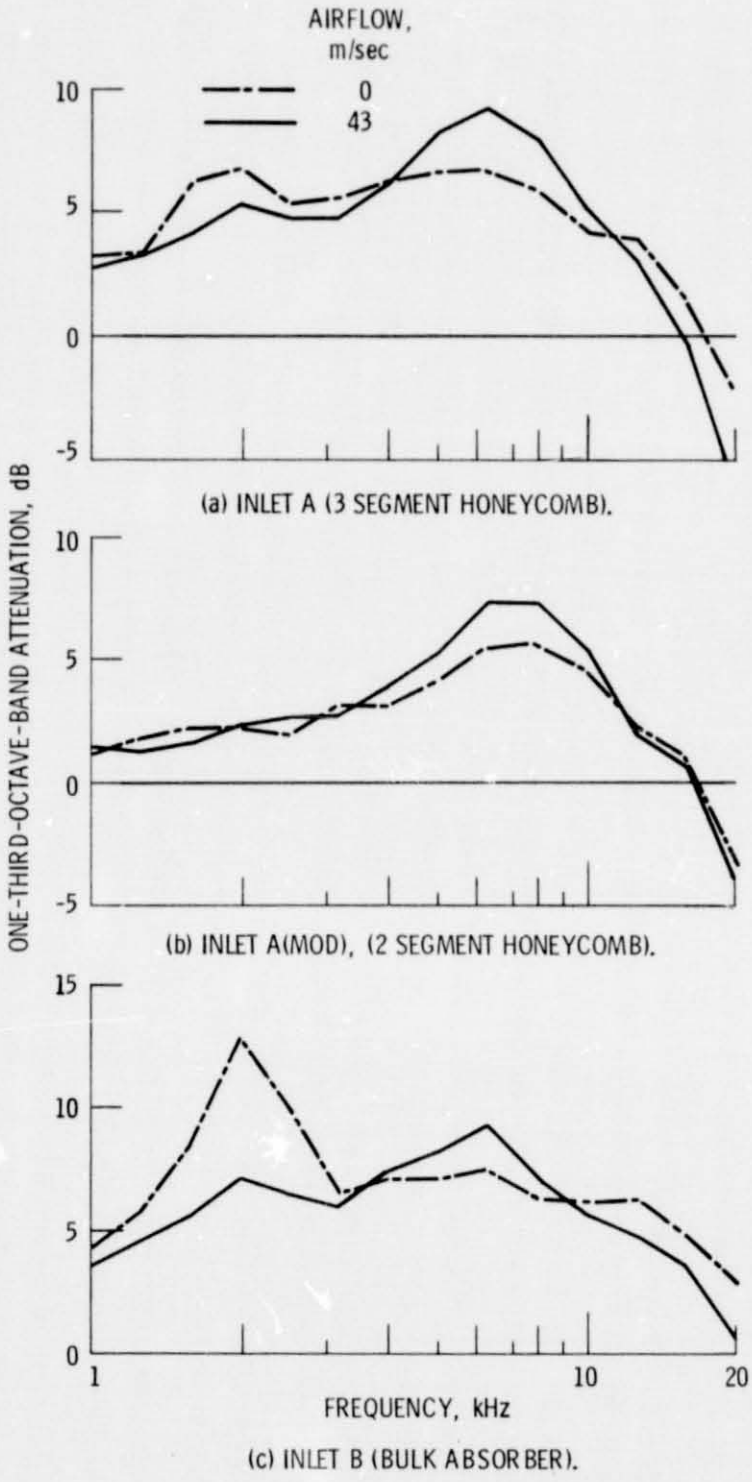

Figure 19. - Effect of tunnel flow on attentuation levels averaged over 95, 106, and 110 percent fan speeds and 60^0 and 90^0 inlet angles.

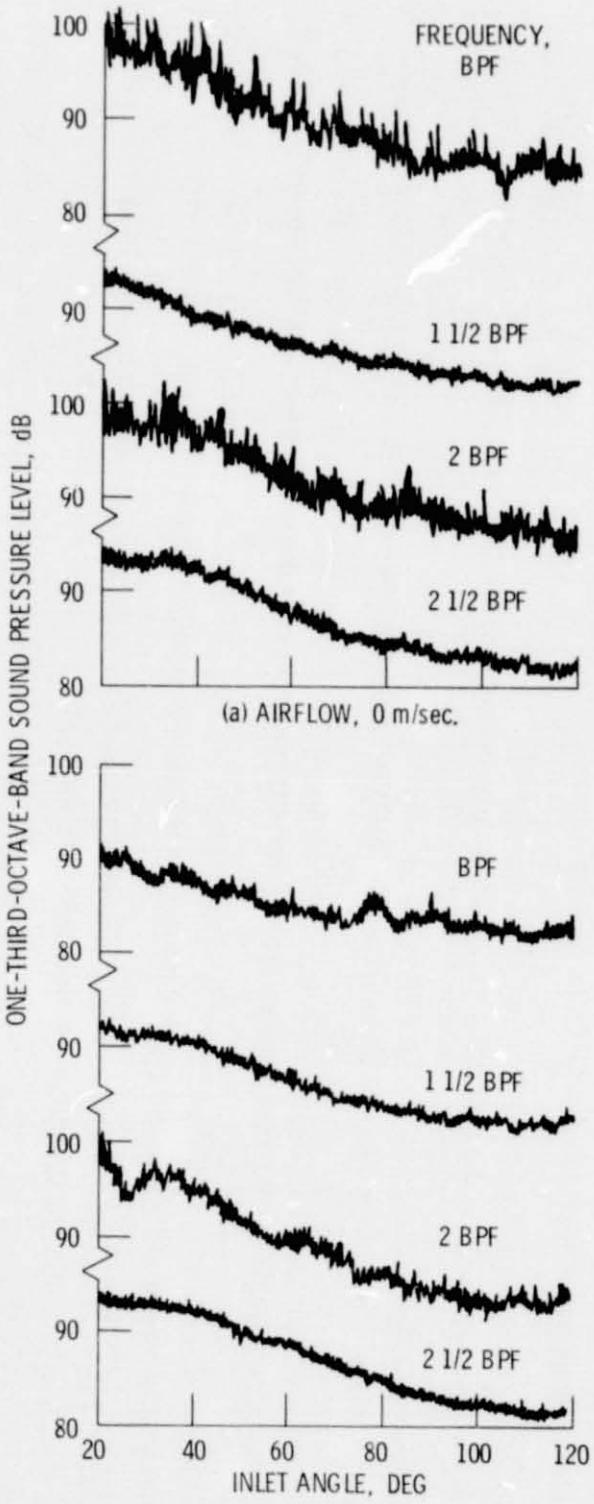

Figure 20. - Inlet B directivity patterns at 106 percent fan speed.

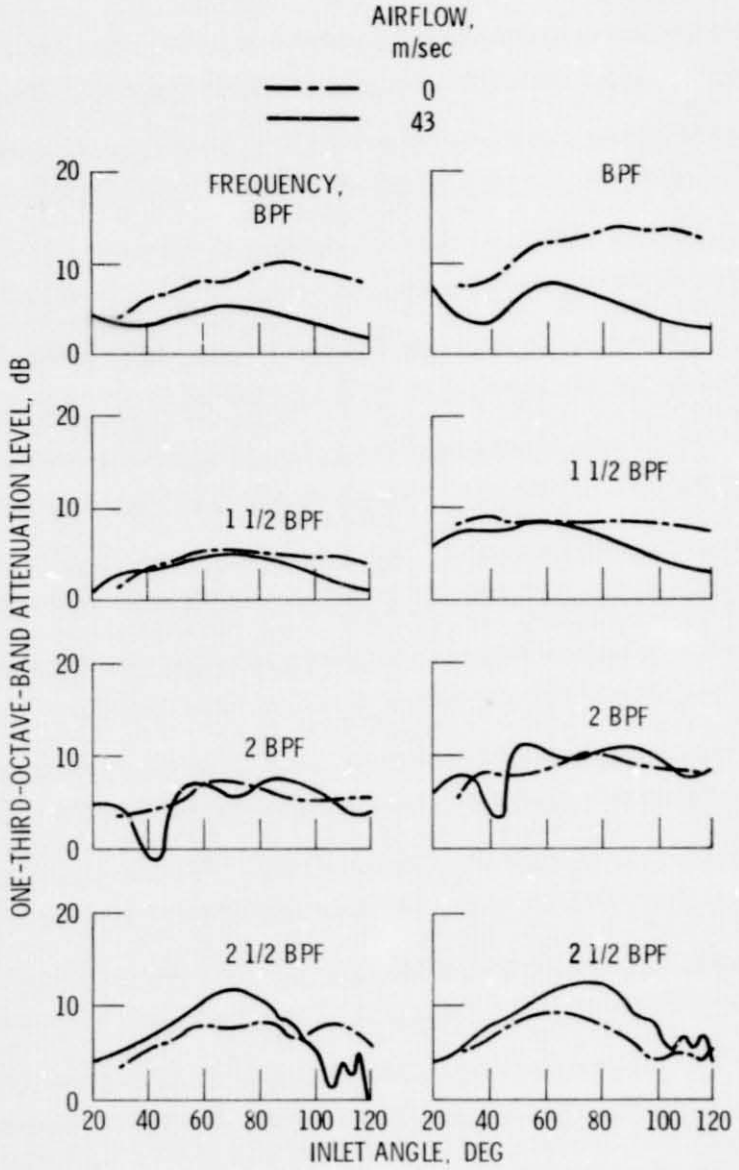

(a) INLET A (3 SEGMENT HONEYCOMB).

(b) INLET B (BULK ABSORBER).

Figure 21. - Attenuation directivites at 95 percent fan speed.

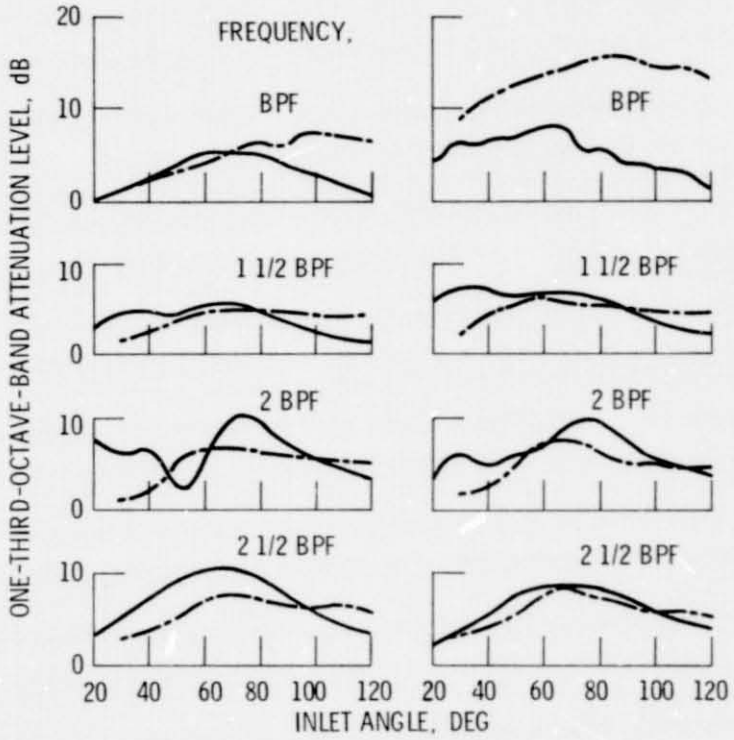

(a) INLET A (3 SEGMENT HONEYCOMB).

(b) INLET B (BULK ABSORBER).

Figure 22. - Attenuation directivities at 106 percent fan speed.

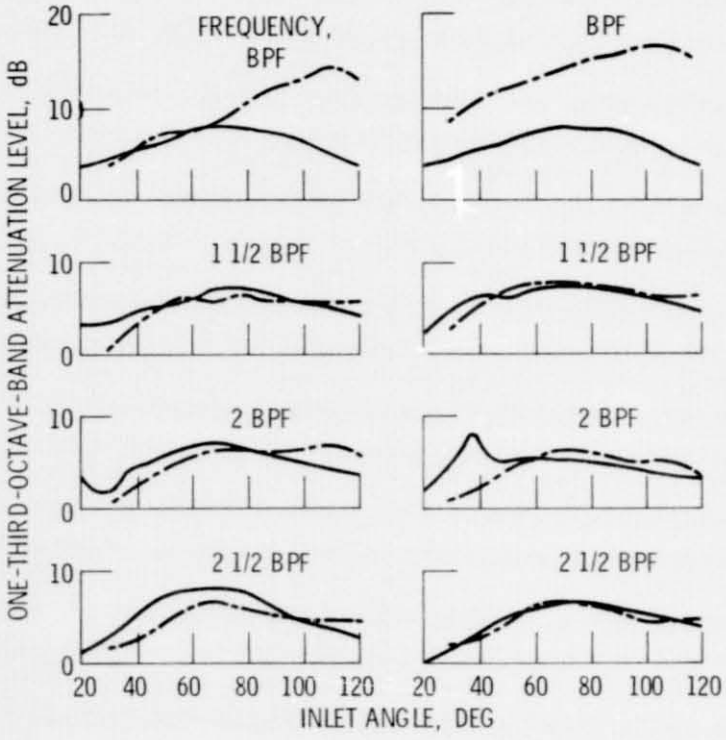

(a) INLET A (3 SEGMENT HONEYCOMB).

(b) INLET B (BULK ABSORBER).

Figure 23. - Attenuation directivities at 110 percent fan speed.

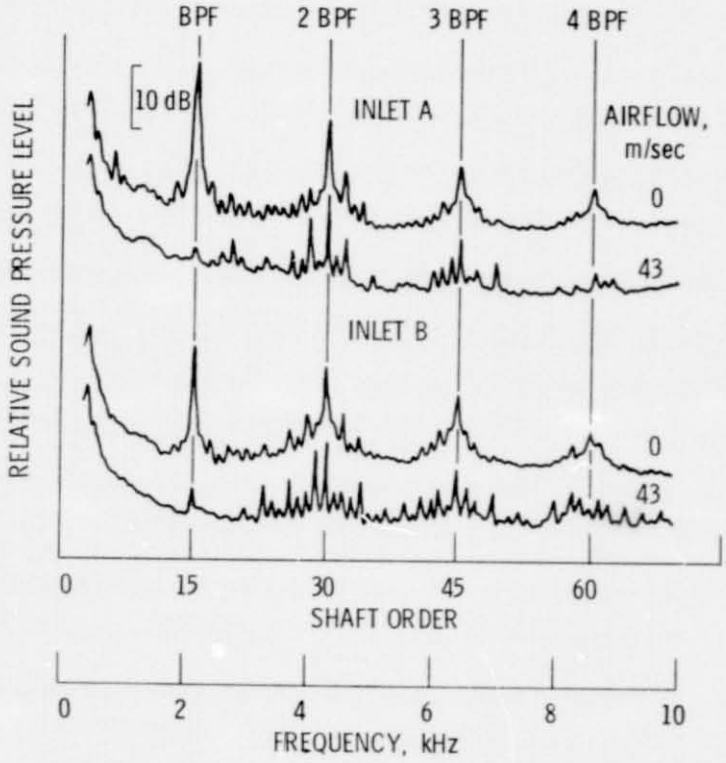

Figure 24. - Inlet A and Inlet B narrowband spectra at 106 percent speed and 60^0 inlet angle.

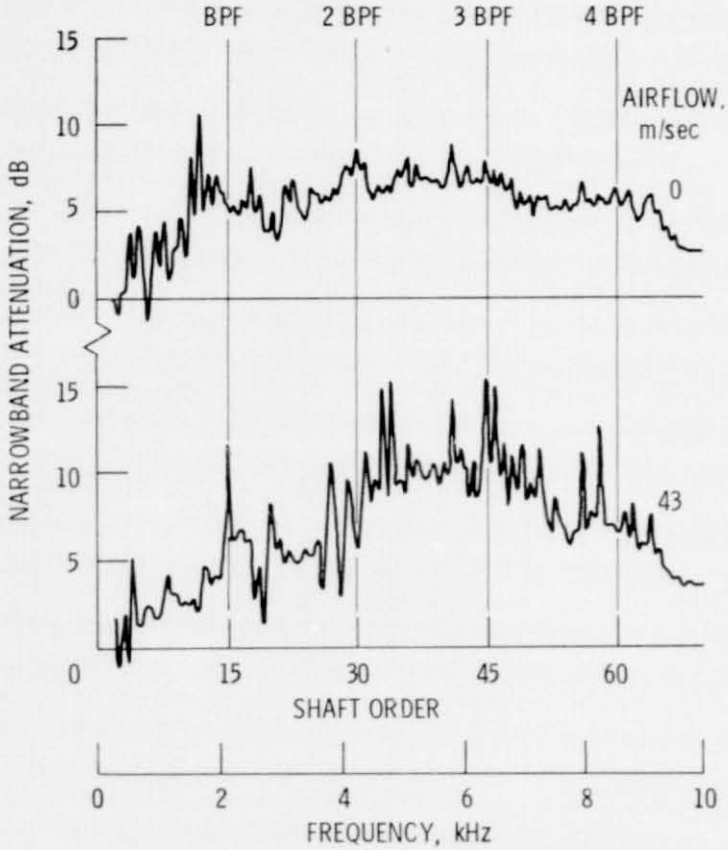

Figure 25. - Inlet A narrowband attenuation spectra at 106 percent fan speed and 60^0 inlet angle.

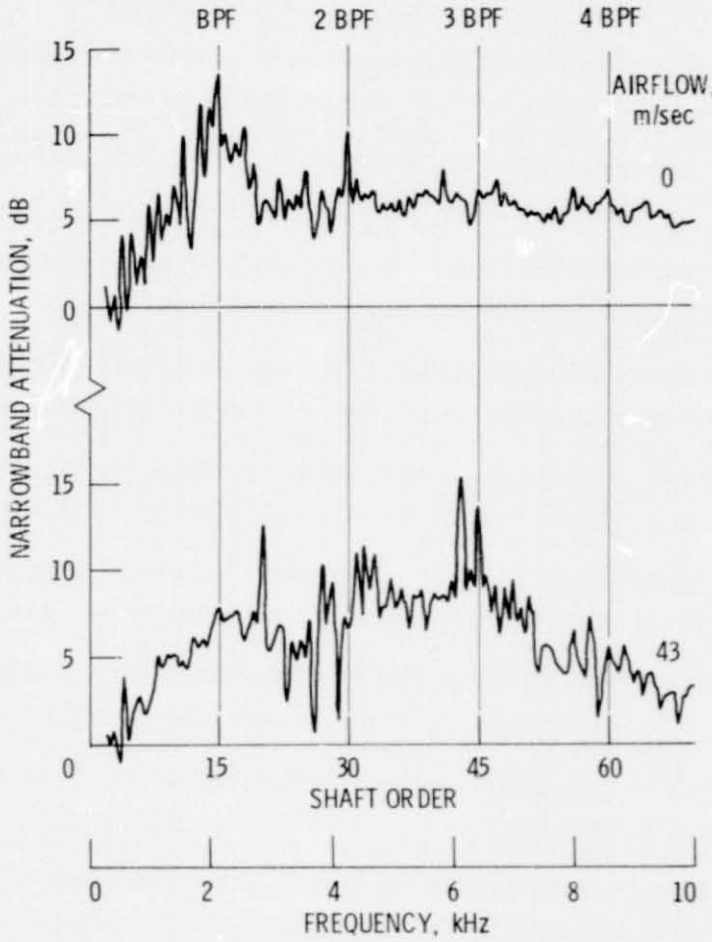

Figure 26. - Inlet B narrowband attenuation spectra at 106 percent fan speed and 60^0 inlet angle.

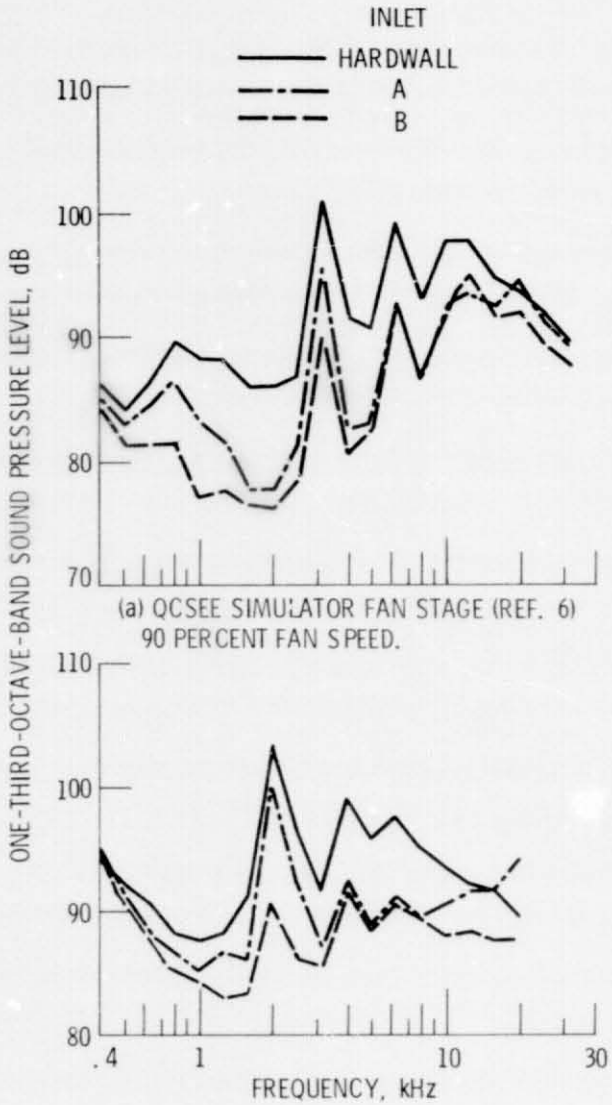

(a) QCSEE SIMULATOR FAN STAGE (REF. 6) 90 PERCENT FAN SPEED.

(b) NASA ROTOR 55 FAN STAGE, 106 PERCENT FAN SPEED.

Figure 27. - Hardwall, Inlet A and Inlet B far-field spectral properties at 60^0 inlet angle with two different fan stages under static test conditions.

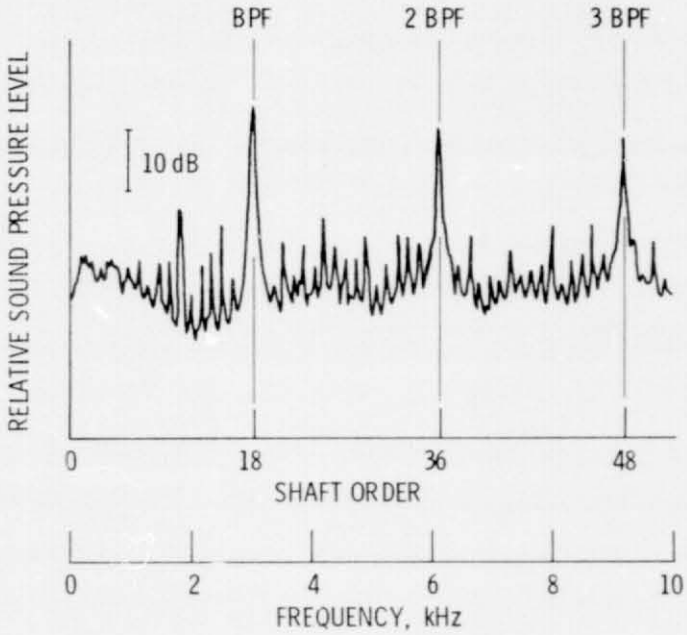

Figure 28. - Narrowband spectra of QCSEE simulator fan stage with hardwall inlet at 90 percent fan speed and 60^0 inlet angle (ref. 6).

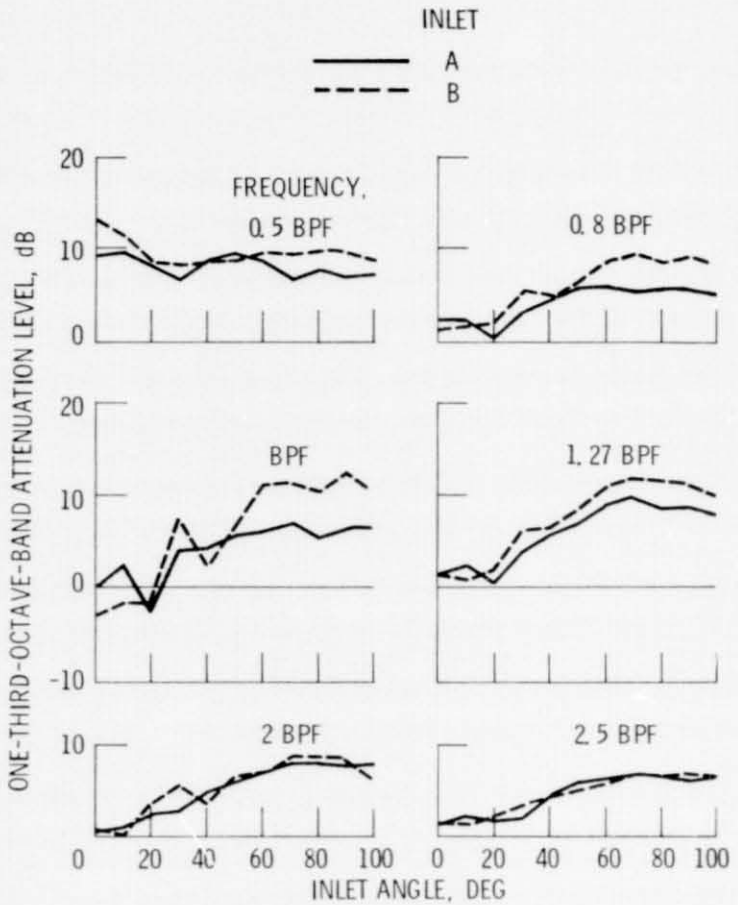

Figure 29. - Inlet A and Inlet B attenuation directivities obtained with QCSEE simulator fan stage (ref. 6) under static test conditions.

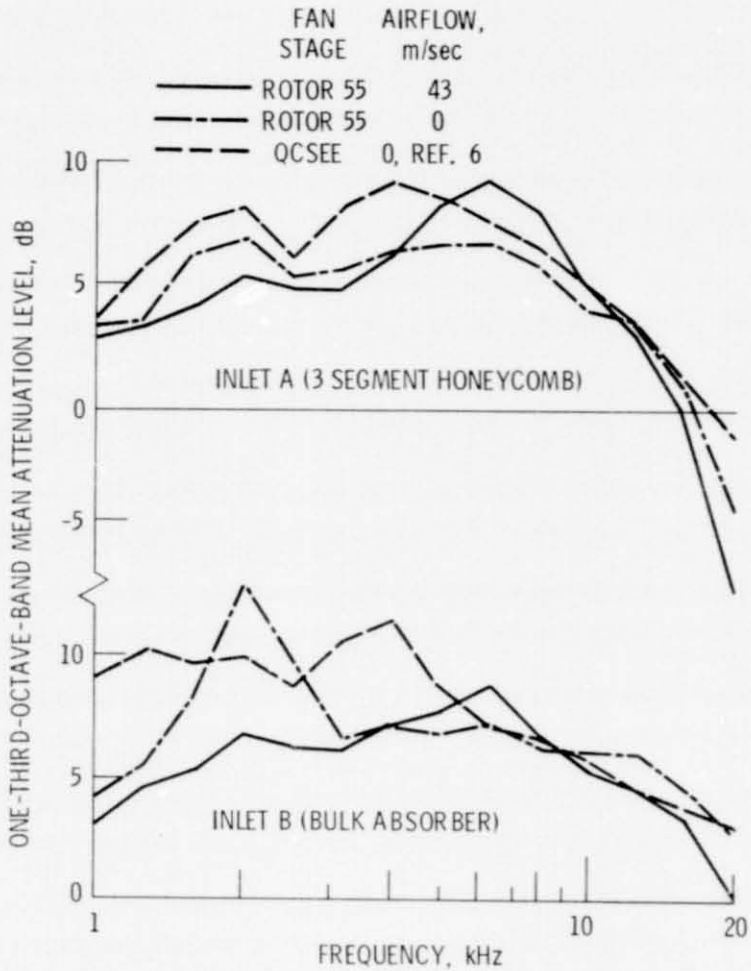

Figure 30. - Comparison of mean attenuation levels obtained with QCSEE simulator and rotor 55 fan stages.